이학 석사 학위 논문

# Comparison and Evaluation of Turbulent Heat Fluxes from Global Reanalysis Products Based on Buoy Observation in the East-Asian Marginal Seas

# 동아시아 연해에서 부이 자료를 이용한 재분석장 비교 검증

2013 년 2 월

서울대학교 대학원

지구환경과학부

정 욱 재

**Comparison and Evaluation of Turbulent Heat Fluxes from Global Reanalysis Products based on Buoy Observation in the East-Asian Marginal Seas**

**동아시아 연해에서 부이 자료를 이용한 재분석장 비교 검증**

**지도 교수 장 경 일**
**이 논문을 이학석사 학위논문으로 제출함**
**2013 년 2 월**

**서울대학교 대학원**
**지구환경과학부**
**정 욱 재**

**정욱재의 이학석사 학위 논문을 인준함**

**2013 년 2 월**

**위 원 장_____**

**부위원장_____**

**위 원_____**

**Abstract**

Determination of accurate quantitative description of mean and variability of ocean surface turbulent heat fluxes is pivotal for understanding and modeling air-sea interactions. Oceanic reanalyses have been very useful in evaluating models, but the quality of these products has often been questioned for specific type of applications. Meteorological variables measured from 6 ocean buoys are used to calculate the latent and sensible heat fluxes with Coupled Ocean-Atmosphere Response Experiment (COARE) flux algorithm 3.0 (Fairall et al., 1996) over the East Asian Marginal Seas. The buoy-derived latent and sensible heat fluxes are compared with those from five atmospheric reanalyses (NCEP1, NCEP2, CFSR, ERA Interim, and MERRA) and objectively analyzed data (OAflux) for evaluation of the products. There exist significant mean biases of the products over the coastal region but relatively small biases in offshore region. NCEP significantly overestimates turbulent heat fluxes all over the region, otherwise MERRA always has the lowest mean values compared to other products, so slightly overestimate or even underestimate the fluxes at which other products show significant overestimation. All products simulate well day to day variation (correlation is higher than 0.83), but the amplitude of variation (in terms of the standard deviation) is better in an order of MERRA-OAflux-ERA Interim-CFSF-NCEP1-NCEP2. This order of performance is nearly same at all buoy stations. In general, heat flux bias comes from two sources; one is algorithm-caused bias and the other is variable-caused bias. This study focuses on the variable-caused bias by applying the COARE 3.0 flux algorithm to bulk variables from all the reanalysis products and performing tests to identify the sensitivity of biases to a single variable or pairs of variables The sensitivity tests suggest that the mean biases of latent and sensible heat fluxes can be improved within an acceptable error range (<10 W/m2) by using high-quality SST observations in the East Asian Marginal Seas.

**Contents**

## List of figures

Figure 6. Scatter plots of daily mean latent heat fluxes derived from buoy observation (x-axis) and from each reanalysis product (y-axis). Linear regression line ( red) and the 1 to 1 line (black) are shown.

Figure 7. Seasonal variation of latent heat flux ($\mathrm{W}/m^2$) based on buoy observation (thick black line), and mean differences of product's latent heat flux with observation (colors). Positive (negative) values of the difference denote the latent flux from the product overestimates (underestimates) the flux.

Figure 8. Same as Fig. 6 for sensible heat flux ($\mathrm{W}/m^2$).

Figure 9. Sensitive test of various combinations (Wind, SST, $\boldsymbol{q_a}$, wind-$\boldsymbol{q_a}$, SST-$\boldsymbol{q_a}$ wind-SST) of these variables to figure out which variable or combination of variables can reduce the latent heat flux difference ($\mathrm{W}/m^2$).

Figure 10. Sensitive test of various combinations (Wind, SST, $\boldsymbol{T_a}$, wind-$\boldsymbol{T_a}$, SST-$\boldsymbol{T_a}$, wind SST) of these variables to figure out which variable or combination of variables can reduce the sensible flux difference ($\mathrm{W}/m^2$).

## List of Tables

## 1. Introduction

The turbulent fluxes of sensible and latent heat transfer heat from ocean to atmosphere (the reverse occurs under rare conditions). The sensible heat (SH) flux is the transfer of heat caused by difference in temperature between ocean and atmosphere, so it raises or lowers air temperature. Although the SH flux is generally small, it can reach a few 100 W/m², where cold wintertime continental air blows over warm ocean. The evaporation of water vapor from the sea surface causes the latent heat (LH) flux. Usually the LH flux is significantly greater than the SH flux, and it is considered to be most important component in air-sea heat fluxes. Turbulent fluxes play a significant role in the exchange of heat and moisture at the air-sea interface, and an accurate determination of mean and variability of turbulent heat fluxes is pivotal for understanding and modeling air-sea interactions (Taylor 2000).

Atmospheric analysis, which is a synthesis of the available observations in the context of a physical model (Trenberth 2010), is one of the widely used turbulent heat flux data. Those analyses, however, are not necessary consistent over long periods because of frequent updates of models and data assimilation methods due to an advancement of technology. In order to reduce the long-term biases, reanalysis data are produced that are based on the same model and a constant state-of--art data assimilation system over the whole period. The reanalysis data provide a long and consistent heat flux data with good global coverage. There are various reanalysis products currently available; these are classified three generation (Trenberth 2010). The first generation, NCEP1 (Kalnay et al. 1996), NCEP2 (Kanamitsu et al., 2000), ECMWF ERA 15 (Gibson et al. 1997), the second generation, ECMWF ERA 40 (Uppala et al., 2005), JRA-25 (Onogi et al., 2007), and recent new generation of several ocean surface heat flux products such as ERA Interim (Dee et al. 2011), CFSR (Saha et al., 2010), and MERRA (Rienecker et al., 2011). A briefly description of products used in this study is given in the next section

However the problem is that it is unclear which dataset provides most accurate representation of surface turbulent heat fluxes (Sun et al. 2003). Then, where does this difference in products performance come from? Or why is it difficult to obtain the flux right? To answer this question, we need to know how to estimate the turbulence heat flux first.

Turbulent heat flux is calculated by using bulk formula, which is parameterization of heat flux based upon Monin-Obukhov similarity theory (Foken 2006), with input variables such as skin sea surface temperature, wind at 10 m height , and specific humidity andair temperature at 2 m height [Liu et al. 1979, Fairall et al. 1996b, Brunke et al. 2003]. The general form of the bulk formula to calculate the latent ($Q_{LH}$) and sensible ($Q_{SH}$) is

$$Q_{LH} = \rho L_e C_e (q_s - q_a)\mathrm{U} \quad (1)$$

$$Q_{SH} = \rho C_p C_h (T_s - T_a)\mathrm{U} \quad (2)$$

where $\rho$: density of air, $L_e$: latent heat of evaporation, $C_e$: turbulent exchange coefficient for latent heat flux, $q_s$: surface specific humidity, $q_a$: near- surface specific humidity, U: wind speed, $C_p$: specific heat capacity of air at constant pressure, $C_h$: turbulent exchange coefficient for sensible heat flux, $T_s$: sea surface skin temperature, $T_a$: near surface air temperature.

Bulk flux algorithms differ in how they parameterize turbulent exchange coefficients ($C_e, C_h$). The coefficients are determined empirically from field experiments, for instance, TOGA-COARE experiment (Weller et al. 1996). There are several forms of bulk flux algorithms currently available (Zeng et al. 1998, Brunke et al. 2003), and different reanalysis products often adopt different algorithms. The estimated values of heat flux are also dependent on the quality and time resolution of input variables, since there are measurement errors and model errors that include uncertainties from the physical parameterizations other than the surface flux algorithm and errors in assimilation of data. Hence, different algorithms and different input variables contribute to the difference in heat fluxes among different

reanalysis products. It has also been noted that if climate conditions in a region differ from those in which the parameterization was developed, it is not guaranteed the same parameterization would hold in the region (Chelton 2001). Hence, even if successful validation was made in one place, careful evaluation is needed to quantify reanalysis flux data at a ‘‘new’’ location/region of interest (Sun et al. 2001).

Direct measurements of turbulent heat fluxes are possible using fast response instruments. Results from those measurements have been used in developing, calibrating, and verifying the turbulent heat flux products (References). However, there is a very limited number of such data available over a wider area. While turbulent flux from flux algorithm with buoy bulk variable is recommended, even though it may be less reliable than direct measurements because of uncertainty of bulk algorithm, since if bulk algorithm is enough evaluated, buoy turbulent heat fluxes can have an accuracy of approximately 10W$m^2$(Payne et al., 2002). It can also provide long, continuous, high-quality air sea flux time series, so these data sets are being used consistently to compare gridded data (Renfrew et al., 2002,Sun et al., 2003, Jiang et al., 2005, Kubota et al., 2008, Shawn et al., 2011). Renfrew(2002) found there were large differences between the observed and NCEP reanalysis turbulent heat flux, especially during the high heat flux due to different heat and moisture roughness length formulations and this is most acute when air sea temperature different are large. Renfrew also suggest recalculating flux with appropriate bulk algorithm and reanalysis bulk variable can reduce the disagreement in fluxes. Sun (2003) report the significant bias in SST analyses in the coastal regions of the western North Atlantic largely affects the magnitude of air sea heat-heat exchange in NCEP1, NCEP2 and ERA40. Sun (2003) and Jiang (2005) showed that the COARE 3.0 algorithm and the reanalysis bulk variables together improved mean turbulent heat fluxes of NCEP2 and ERA40 by reducing mean biases. Kubota (2008) examined the differences between COARE algorithm and the study by Kondo (1975), and found the

discrepancies between these bulk algorithms are important only when discussing the accuracy of global LH flux in quantitative detail. Shawn (2011) report that Global comparisons of monthly means tend to reveal similar spatial patterns in turbulent heat flux; however, the magnitudes and patterns of variability are widely different. While Basin scale and regional analysis further reveals large differences.

The East Asian marginal seas are composed by three Seas: Yellow Sea, The East/Japan Sea, and East China Sea (Korea straits). The Yellow Sea is a semi-enclosed basin located between China and Korean peninsula with the Bohai Sea to the northwest and the East China Sea to the south. Yellow Sea is shallow sea, a maximum depth of about 140 m and most of the area is less than 50m, therefore it will be readily affected by seasonally varying atmospheric conditions such as heating, cooling, and wind stress. During the summer the warm and weak wind blows to the north, and generates a large difference between air temperature and SST, a highly stable marine boundary layer (Chu et al. 2005). The East Sea is a semi-enclosed ocean basin surrounded by four countries of South Korea, North Korea, Russia and Japan. The East Sea is subjected to the seasonal monsoon system. During the winter monsoon, from November through April, a cold northwest wind blows over the East Sea. During the summer monsoon, from mid-May to mid- September, a weaker southeasterly wind blows over the East Sea (Chu et al., 2001).

The meteorological variables used herein were collected from five ocean buoys [Dukjukdo (DJ), Chillbaldo (CB), Keomundo (KM), Keojedo (KJ) and Donghae(DH)], which have been operated by the Korea Meteorological Administration (KMA) since 1997, and Yellow Sea Monitoring Buoy (YB), which has been operated by the Korea Ocean Research Development Institute (KORDI) since 2007. Detailed information of these observation data is shown in Fig. 1 and listed in Table 1. DJ, CB and YS represent of Yellow Sea, KM and KJ represent of Korea Strait, and DH represent of East Sea.

The studies of heat flux in the East Asian marginal seas are mainly focused to figure out characteristic of air-sea exchange by using climatological means or statistical methods, and most of the studies are limited to the East/Japan Sea area due to relative abundance of observations (Na et al., 1999). Our study complements and extends these previous studies-comparing the latent and sensible heat fluxes derived from the reanalysis products and directly measured variables by ocean buoys and including new reanalysis data (ERA-Interim, CFSR, MERRA) in the comparisons as a benchmark for evaluating the other products in the East Asian marginal seas. We focus on the variable-caused biases by calculating (or recalculating for some of reanalysis products) those fluxes using the same COARE algorithm. There exists few direct turbulent flux measurements in the region to evaluate the algorithm-caused biases.

This study is organized as follows, Brief description of reanalyses data and the basic characteristics of in situ measurements with processing procedure in section 2, evaluation of mean and variability of the daily flux product at in situ measurement sites section 3, and discussions of whether it is possible to improve products flux with respect to already existing products in section 4.

## 2. Data and processing

### 2.1 Reanalysis data

A brief summary of the reanalysis products

a. ERA-Interim

ERA-Interim is the latest generation of ECMWF reanalyses from 1979 to present, continuing with monthly updates (Uppala et al. 2005). It provides 6-hourly upper-air, 3-hourly surface, monthly averages and diagnostics products which is available at www.ecmwf.int/research/era. The main object of the ERA-Interim is to replace ECMWF's previous reanalysis ERA-40 (1957 -2002). There are several differences between ERA-Interim and ERA-40 in data assimilation and observing system. The assimilating model is the ECMWF Integrated Forecast Cy31r2 (Dec 2006) with a higher horizontal resolution (T255) and 60 levels in the vertical, with the model top at 0.1hPa. The main improvements in the ERA-Interim analysis method compared to ERA-40 are 4D-Var with 12-hour analysis window, the use of variational bias correction for satellite radiances, static background error covariance using wavelets, and 1D +4 D-Var assimilation of SSM/I rain-affected radiances. ERA-Interim uses input observations prepared for ERA-40 until 2002, but data from ECMWF's operational archive thereafter such as direct assimilation of SSM/I clear-sky radiation from Meteosat-2 and use of SSM/I rain –affected radiances. SST was taken from the different products; prior to 2001 as in ERA-40(HadISST1 then NCEP) and after 2001 as in IFS (NCEP then OSTIA).

d. OAFlux

OAflux is not a reanalysis product but kind of hybrid product. OAFlux is developed by the objectively Analyzed air-sea Heat Fluxes (OAFlux) project at the Woods Hole Oceanographic Institution (WHOI). It applies objective analysis approach to obtain the best possible surface variables which is used to calculate turbulent heat fluxes (Yu and Weller 2007). They are constructed not from a single data source, but from an optimal blending of satellite retrievals

(scatterometer and radiometer, SSMI and AMSR-E) and tree atmospheric reanalyses (NCEP1, NCEP2 and ERA 40). Through this, the strengths of several in situ or satellite data sets and NWP analysis are combined. The optimally estimated variables are then utilized to compute daily flux fields from the COARE bulk flux algorithm3.0. OAFlux currently provides global heat flux data and ocean evaporation from 1958 to 2008 with a spatial resolution of 1° at http://oaflux.whoi.edu/.

**2.2 Averaging issues and Matchup Procedure**

A fair comparison of fluxes based on data from buoys and products is not an easy task because of the differences in 1) time intervals, 2) spatial resolutions, and 3) flux algorithms. Data intervals of the reanalysis products are different, varying from hourly (MERRA) to daily (OAFlux), and the buoy data at all stations were obtained on an hourly basis. We calculated the heat fluxes using the original bulk variables with different time intervals based on the COARE algorithm. The calculated fluxes in an interval shorter than one day are then daily averaged. Systematic errors can be potentially introduced in averaging the fluxes depending on averaging methods. Brunke et al (2011) addressed that the averaging procedure does not introduce any systematic reduction or amplification of biases for products (MEMRRA, CFSR, and ERA-Interim) with different temporal resolutions but the standard deviation generally decreases as the averaging period increases. For this reason, it is needed to check the results presented in the present manuscript did not significantly differ according to the averaging period. 2) Buoy measurement is a single point data while model products are gridded data with spatial resolutions of 0.5°~1.825°. Model's coarse spatial resolution can lead to contamination from land since most of buoys are located close to coast. To match buoy data with gridded products, first we removed grid point which contains a fraction of land in grid box by using land/sea mask provided by each product (i.e., MERRA land/sea mask base on

the 1km Global Land Cover Characteristics (GLCC) database). Next we used bilinear interpolation with the surrounding four grid points around the buoy position or just chose the nearest grid point to the buoy location to avoid grids including land. The latter was the case for the reanalysis products having low spatial resolution such as NCEP1 and NCEP2. The reanalysis products can be thought as area averages; hence a certain amount of spatial variance would be smoothed out. This smoothing effect can be significant in coastal regions where oceanic and atmospheric fields change abruptly in space that the products cannot resolve properly (Taylor 2001). Four stations among the six ocean buoy stations are located close to the coast within 44 km from the nearest coastline. The influence of the proximity of the buoy stations to the coast in the comparison of heat fluxes will be discussed in Section 4. 3) The Coupled Ocean-Atmosphere Response Experiment (COARE) bulk flux algorithm 3.0 (Fairall et al. 2003) is used to calculate latent and sensible heat fluxes based on data from ocean buoys. The COARE algorithm was one of the least problematic of 12 bulk algorithms in the Tropical Pacific (Brunke et al. 2003).The COARE algorithm, however, has not been validated in these East Asian marginal seas, to the best of our knowledge. We assume that it is the more accurate bulk algorithm, different flux products were compared to each other on buoy flux basis. This study, however, does not address the algorithm-caused biases because of the lack of directly measured turbulent flux data, but focuses on the variable-caused biases.

We adopted the quality check method suggested by Hiroese et al. (1996); after removal of the obvious bad data points, individual values beyond three times standard deviation from the mean for each month are considered as the spikes and removed from the raw data. Bulk variables measured at heights ranging from 3.3 m to 4.8 m are adjusted to the reference height (10 m for wind, 2 m for relative humidity (Rh) and air temperature (Ta)) for comparison with products. The specific humidity at buoy stations ($q_a$) is determined from the relative humidity and Ta using TeTen's formula (Bolton 1980). Sea surface temperature (SST)

at buoy stations was measured at about 1 m depth, hence, represents bulk sea surface temperature, so it needs to be converted to skin temperature. The difference between bulk sea surface temperature and skin temperature can result in systematic errors larger than 10% of the computed fluxes (Curry et al. 2004). However, we did not convert the measured bulk sea surface temperature to skin sea surface temperature due to the lack of downward longwave and shortwave fluxes. According to Park (2008), who compared NOAA/AVHRR SST and in situ temperature measurement, the difference between the skin and bulk SST in the East Asian seas has a 0.185℃ of bias. The effects on this difference are amount of 2~4.5 $Wm^2$ for latent heat flux and 1~2 $Wm^2$ for sensible heat flux (Table. 5). In COARE algorithm, wind speed in equation (1), (2) denotes wind speed relative to surface current speed (U=$U_{air}$-$U_s$, Fairall et al. 2003). However, no surface current data was available in KMA buoys. So, $U_s$ was taken to be zero. This is same as in NCEP1 and NCEP2. Such an assumption, however, could lead to significant errors in regions with strong currents (Jiang et al. 2005).

Because of above constraints, careful attention is required to interpret results correctly. However, in spite of these limitations, KMA and KORDI buoy data have merits in that special attention should be given to marginal sea areas, where available flux products are no using suitable parameterizations and the coarse spatial resolution leads to contamination from land observations (Taylor et al. 2001) and KMA and KORDI buoy data are not used either for validating bulk algorithms or directly as inputs of these algorithms.

## 3. Results

### 3.1 Comparisons with buoy

For the accurate quantitative description of mean and variability of turbulent heat fluxes, two common types of errors are analyzed: system errors that bias the mean and random errors that influence the variance.

#### 3.1.1 Long term mean bias

Fig. 2(left) shows total mean bias based on the daily mean LH flux at six buoy stations. Considering missing data from buoys and different observation periods, the averages are taken by using all available data at each buoy station (Table. 2). Positive value in y-axis means that the reanalysis products overestimate the fluxes (more heat loss) as compared to the fluxes based on the buoy observation. The results in Fig. 2(left) indicate that the deviation between heat fluxes from the products and observation vary depending on regions and products selected.

**a. Mean**

At first four sites (DJ, CB, KM, KJ), closer to the land boundary within (~44 km) and shallower depths (<~80 m), all of the products except MERRA tend to overestimate latent heat flux. Especially, the reanalysis products significantly overestimate the LH at sites CB and KM; the mean biases at CB and KM are in the range of 24~58 $W/m^2$ and 24~83$W/m^2$, respectively, which correspond to 56~135% at CB and 31~103% of the mean LH fluxes from buoy observations. This comparison poses a significant problem for the use of reanalysis products in coastal region as expected. The analysis products slightly overestimate or underestimate the LH fluxes at offshore stations, DH and YS;-28 (25%) ~ 11.4 (10%) at DH and -19.3 (22%) ~ 20.6 (24%) at YS.

NCEP2 has the largest mean biases at all sites, and they are larger than twice the mean LH

fluxes at CB and KM. NCEP1 also overestimates the LH fluxes, but shows a better performance than NCPE2 which is an update version of NCPE1. The overestimation of LH flux for NCEP products has been previously documented as well (Sun et al., 2003, Jiang et al., 2005, Kubota eat al 2009). The performance of CFSR, the latest product of NCEP is similar to those of NCEP1 and NCEP2 in coastal region. However it has better performance at offshore sites. MERRA always has the lowest mean LH fluxes compared to the LH fluxes from other products at all sites, Hence, the comparison of LH fluxes between MERRA and observation shows underestimation at offshore sites and relatively small overestimation (less than $8\,\mathrm{W}/m^2$) at coastal sites. ERA-Interim shows the best performance throughout the all location in terms of mean bias, but has large biases at CB and KM. OAFlux shows large biases at CB and KM. OAFlux uses the same bulk algorithm, COARE 3.0, as that is used to calculate fluxes from buoy data, hence the biases then would be caused by input variables.

**b. Variation**

Taylor diagram (Taylor, 2001) is used to illustrate the relative accuracy of demeaned temporal variability amongst LH fluxes from various reanalysis products as compared to the observation (Fig. 3, Case A). Taylor diagram relies on three non-dimensional statistics; the correlation and the centered root-mean–square (RMS) difference between the two fields, and the ratio of the variance of the two fields to be compared. The ratio of variance indicates the relative amplitude of the observed field (LH flux based on buoy data) and the reanalysis field (LH flux from each of the products), whereas the correlation indicates whether the fields have similar patterns of variation, regardless of amplitude. The three statistics are related by following formula, $E'^2 = \sigma_f^2 + \sigma_r^2 - 2\sigma_f\sigma_r R$, where R is the correlation coefficient, E' is the centered RMS difference, and $\sigma_f$ and $\sigma_r$ are the variance of the products and buoy data. The product that agrees well with observed variability will lie nearest the point marked 'REF',

representing the observation, on the x-axis and (Taylor 2001). ERA-Interim, CFSR, and OAFlux, are very close each other on Taylor diagram, indicating that they have a similar pattern of variation. For those products, the distances to the REF are short in most cases in Fig.3, while NCEP1 and NCEP2 lie remote from REF at all sites, indicating the temporal variation of LH fluxes from NCEP1 and NCEP2 is much different from those based on buoy observation.

In spite of large mean biases, all products have high correlation coefficients (0.83~0.97) with even higher correlation (>0.95) at offshore sites. The relative amplitude of variation (represented by standard deviation, STD, in the figure), however, varies from place to place but with a common feature in terms of the magnitude of amplitude amongst products. For NCEP1 and NCEP2, the amplitudes of the variation are much larger than those from other products at all sites. On the other hand, the flux calculated from MERRA has the smallest standard deviation at all sites, and the standard deviations of the LH fluxes from the other products (ERA-Interim, CFSR and OAFlux) lie between MERRA and NCPE1. As a result, as shown in Fig.4, all of LH flux products have about the same correlation but due to large standard deviation magnitude in NCEP1 and NCEP2, it make NCEP1 and NCPE2 have largest RMS difference (30.7~78.8 W$m^2$ for NCEP1, 38.2~95.8 W$m^2$ for NCEP2) over the whole region, considering above relationship between RMS, STD and correlation. MERRA has relatively lower RMS differences (29.8~47.4 W$m^2$) except 65.8 W$m^2$ at KJ. ERA-Interim, CFSR and OAFlux also have a similar magnitude of RMS difference (19.6~53.8 W$m^2$ for ERA-Interim, ~49.3 W$m^2$ for CFSR, 22.9~54.7 W$m^2$ for OAFlux.

Mean biases of SH fluxes range from -9.7 W/m^2 to 36.3 W/$m^2$, corresponding to 73.4~208% of mean bases, hence the mean bias of the SH flux at all sites are also significant (Fig, 2 left). Mean bias and variation pattern of SH fluxes are quite similar to LH fluxes; relatively large bias at the coastal region and distribution on the Taylor diagram (Fig 4 Case

A).

### 3.1.2 Variable caused bias

The above comparison highlights significant errors of LH and SH fluxes from the reanalysis products examined, especially at coastal sites of the eastern Yellow Sea. As different flux algorithms are adopted in different products, the errors could be due to the difference in the algorithms as well as errors in variables. To identify the algorithm error, direct measurements of turbulent heat fluxes are required as in Brunke (2011). These are currently unavailable in the study region, and our focus is on the errors due to the bulk variables. We recalculates turbulent heat fluxes using the COARE algorithm with bulk variables from all reanalysis products. We refer to these recalculated heat fluxes with suffix 'C', like NCEP1C and MERRAC as in Jiang (2005). The COARE algorithm was used in calculating the LH and SH fluxes based on buoy data in the above section.

**a. Mean**

Fig.2 (right) shows the difference in LH fluxes between those from reanalysis products recalculated by using the COARE algorithm and derived from buoy data also with the COARE algorithm (referred to as RECALD hereafter, while the difference in LH fluxes between those based on original algorithms of the reanalysis products and derived from buoy data with the COARE algorithm shown in Fig. 2(left) are referred to as ORID). The difference between RECALD and ORID (RECALD minus ORID) shows negative values for NCEP1, NCEP2, CFSR, and MERRA at all sites (Table 5 and 6). The minus sign means that the LH and SH fluxes are reduced (less heat loss from the ocean's surface) when the COARE is used instead of using the original bulk formulae algorithm for each reanalysis product. It then indicates that the mean biases are reduced for those products which overestimated the fluxes with original algorithms (Fig. 2), while the change to the COARE algorithm underestimates the fluxes even more for the products which underestimated the fluxes with

original algorithms. The former is the case for NCEP1, NCEP2, and MERRA at coastal sites CB and KM. Large positive mean biases of heat fluxes at these sites (Fig. 2, left) are drastically reduced when the fluxes are recalculated with the COARE algorithm(Fig. 2 right); the mean bias of the LH flux is reduced by 25.6~ 47.4 $\mathrm{W}/m^2$ for NCEP1, 26.3 ~ 46.2 $\mathrm{W}/m^2$ for NCEP2, and 17.4 ~ 17.3 $\mathrm{W}/m^2$ for MERRA (Table 5). Recalculated LH fluxes for MERRA and NCEP1 now become acceptable (< 10 $\mathrm{W}/m^2$) as compared to the fluxes based on buoy data, but the recalculated LH fluxes for NCEP2 still significantly overestimates the fluxes. The recalculation with the COARE algorithm for NCEP1 and MERRA, however, now underestimates the LH fluxes significantly at site KJ and offshore sites DH and YS with lesser extent for NCEP2. There The algorithm change to COARE also results in the reduction of the difference between RECALD and ORID for CFSR at all sites but with lesser extent (0.2 ~ 11.5 $\mathrm{W}/m^2$) as compared to those for NCEP1, NCEP2, and MERRA (Table 5), indicating CFSR is less sensitive to the change in the algorithm.

The difference between RECALD and ORID shows positive values at all sites for ERA-Interim and OAFlux, indicating the LH and SH fluxes are increased (more heat loss from ocean's surface) when the algorithm switches to the COARE. The OAFlux uses the same COARE algorithm, hence the difference is the smallest. The difference has a range of 3.7~13.4 ($\mathrm{W}/m^2$) for ERA-Interim, hence the absolute difference is smaller than NCEP1, NCEP2, and MERRA and comparable to CFSR (Table 5).

It is difficult to say how much the difference in bulk algorithms used in the reanalysis products contributes to total biases shown in Fig. 2 (right) from the above results, because their algorithms are only compared to COARE 3.0 algorithm. We have not exhaustibly tested the sensitivity of fluxes to different algorithms. However, it is noteworthy that the above analysis indicates that with the same input variables, turbulent heat fluxes calculated by using the COARE3.0 algorithm are reduced as compared to those calculated with original

algorithms used in NCEP1, NCEP2, and MERRA.ERA-Interim and CFSR algorithms behave similar to the COARE 3.0 algorithm at all sites.

**b. Variation**

In Fig 3 and 4, the case A and B show that characteristics of temporal variability of recalculated LH fluxes change little in terms of the amplitude of variation and RMS difference except for NCEP1 and NCEP2, which show reduced amplitude and RMS difference and now become comparable to the observation. MERRAC showed a large reduction in LH and SH fluxes when its algorithm switches to the COARE, but shows relatively small changes in the characteristics of temporal variability.

**3.1.3 Individual bulk variable biases**

Although the mean biases based on recalculated fluxes are reduced at coastal sites, they are still large, up to 114% (ERA-Interim at CB) of the mean fluxes based on buoy data. It suggests the important contribution of the variable caused bias to the large mean bias. This section investigates how the differences of bulk variables (wind speed, air temperature, sea surface temperature, specific humidity) and their combinations (Ts-Ta, Qs-Qa) between those derived in the reanalysis products and directly measured at buoy stations affect the mean biases of recalculated fluxes. The analysis of bulk variable bias can help to improve the variable fields in the reanalysis products. In Fig. 5, all bulk variables from reanalysis products are compared to co-located bulk variables from observation in terms of respective record-length mean values. Positive values in the y-axis in Fig. 5 denote that the bulk variables from the reanalysis products are greater than those directly measured at buoy sites.

**a. Sea surface temperature (SST)**

Fig. 5 shows the difference between the skin temperature from each of reanalysis and bulk SST measured at each buoy site. Mean SST ranges from 13.4 ℃ and 18.4 ℃, and higher mean SST occurs on the path of the Tsushima Current (sites KM, KJ, and DH). Warm

biases of SST are significantly large (0.78~ 2.65℃) at costal sites DJ, CB, and KM. The mean difference between the skin temperature and bulk SST in the East Asian Seas is 0.18℃, but it can be larger near the coast, and the standard deviation of the difference is in range of 0.9~1.2℃ at the eastern boundary of the Yellow Sea (Park, 2008). Even considering this difference between the skin temperature and bulk SST, the warm biases of all products are significantly large at coastal sites of the eastern Yellow Sea, especially at CB and KM (1.79~ 2.65℃). The SST bias at site YS in the Yellow Sea about 177 km off the coast is smaller than 0.3℃. Sun (2003) pointed out the inability of the models' coarse resolution to properly resolve the strong surface temperature gradients along the coastal region contributes to large biases of turbulent heat fluxes in the mid latitude coastal region of the western North Atlantic. There exist strong surface thermal fronts around the buoy stations where large warm biases appear. The fronts are formed due to tidal mixing which acts to vertically mix the water column on the shallower side of the fronts and result in relatively cold coastal SST especially in summer (Choi et al., 1998). In other word, Oceanic dynamic features are important in the formation of surface temperature gradients in this area. The large warm biases at DJ, CB, and KM are considered to be caused by models' coarse spatial resolution unable to resolve regional ocean dynamic feature. Mean SST bias for CFSR is as high as those for other products in spite of its highest resolution with coupled atmosphere-ocean data assimilation. This could be due to still not enough resolution to resolve the small scale coastal frontal features or/and missing dynamics in simulating the tidal mixing.

At site DH in the East Sea, all products underestimate SST, and the mean biases of NCEP1 and NCEP2 are larger than 1℃. Otherwise, mean SST biases for the reanalysis products at offshore sites DH and YS are small.

**b. 2m Air temperature ($T_a$)**

Mean biases of air temperature range from -1.3~ 2.54℃ with relatively large warm biases for all products at CB where the mean bases of SST were also relatively large (Fig. 5). MERRA overestimates the air temperature at all sites especially at coastal sites CB (2.54℃) and DJ (1.47℃) in the eastern Yellow Sea. Except at site CB, air temperatures from ERA-Interim, CFSR, and OAFlux agree with the observation with the magnitude of biases less than 0.11℃ for ERA Interim, 0.42℃ for CFSR, and 0.63℃ for OAFlux. Mean biases of air temperature for NCEP1 and NCEP2 show a similar pattern, cold biases at KJ and KH but warm biases at CB, KM, and YS.

**c. 2m Air specific humidity ($q_a$)**

The near surface specific humidity in all products is, overall, wet biased (up to ~1.33g/kg) except dry biases for ERA-Interim and OAFlux at KM, KJ, and YS. At DJ and CB (Fig. 5). The difference between each of the products and observed specific humidity was quite large in summer when observed mean relative humidity is higher than 80 % due to warm and humid southwest wind (not shown).

**d. 10m Wind speed**

Mean wind speeds at buoy sites range 4.5 m/s to 6.8 m/s with the weakest speeds at sites DJ and CB in the western coast of Korea and the strongest at KM and KJ in the southern coast of Korea (Fig. 5). Sites DJ, CB, YS are all in the open Yellow Sea side and subject to the seasonal monsoon; a cold strong northwest wind in winter and a weak southeast wind in summer. In spite of this regional setting, the coastal sites DJ and CB show the weakest mean wind speeds as compared to those at other sites including the offshore site YS, presumably due to local effects around the buoy sites.

The comparison of wind speeds between each product and the observation can be categorized into two site groups (Fig. 5). Most products overestimate the wind speed at

coastal sites DJ and CB in the Yellow Sea, while underestimate it at other sites along the southern coast of Korea (KM and KJ) and the offshore sites in the East Sea (DH) and in the eastern Yellow Sea (YS). At sites KM, KJ, DH, and YS, the mean biases for ERA-Interim, NCEP2, CFSR, and OAFlux are small while the biases are relatively large for NCEP1 and MERRA. The mean biases for NCEP1 and MERRA were relatively small at sites DJ and CB, indicating that wind speeds for NCEP1 and MERRA are weaker than those from rest of the products to be compared. During the strong wind bursts with speeds higher than 5 m/s, NCEP1 and MERRA significantly underestimate the observation as compared to other products. Hence, the small biases at DJ and CB for NCEP1 and MERRA do not mean their good performance, but rather an evidence of a systematic underestimation of wind speed for MERAA and NCEP1 over the study domain.

**e. Temporal variation of bulk variables**

All products quite well capture the daily variation of bulk variables seen in the buoy observations (not shown). On Taylor diagram, bulk variables (air temperature, SST, air specific humidity) from all products are very close each other at all sites and they all have high correlation and much similar value of RMSE, standard deviation. The similarity is expected to some extent, since sea surface temperatures in most of products are derived from Reynold's SST products, and both air temperature and air specific humidity have a strong dependence on the SST, since 2m air temperature is driven by optimal interpolation with model's lowest level air temperature and surface temperature, and air specific humidity is function of air temperature and pressure. SST and air temperature variations are quite similar to those of saturated specific humidity and specific humidity, respectively. A comprehensive comparison of the observed and modeled surface data is summarized in Table 7~12.

### 3.2 Error characteristic

### 3.2.1 Vertical temperature and moisture gradient

Since $q_s$ is calculated from the saturation humidity for pure water at SST, the bias in SST has a clear effect on the estimates of both vertical temperature and humidity gradients between air and sea. Large warm SST biases result in large overestimates of vertical temperature gradient for most products at sites DJ, CB, KM, and KJ. The biases of vertical temperature gradient are low at DJ and CB, in spite of large mean biases of SST and air temperature Errors in each variable can compensate each other and make the variable combination agree better with the observation.

### 3.2.1 Variable-caused errors in turbulent heat fluxes

In general, bulk variables that cause main errors in turbulent heat fluxes can vary from place to place depending on regional atmospheric and oceanic characteristics, because relationship between the fluxes and the flux related variables is nonlinear. Large variable-caused biases of LH and SH for ERA-Interim, NCEP2, CFSR, and OAFlux at CB and KM in Fig. 3b and Fig. 4b seem to be caused mainly by large warm biases of SST (1.79~ 2.65℃). The bias in SST has clearly an effect on the estimates of both vertical humidity and temperature gradients, and then multiplication of the wind speed with those vertical gradients of moisture and temperature determines the LH and SH fluxes, respectively. The SST biases lead to biases of (0.73~ 2.05g/kg) in vertical humidity gradients and (0.63~ 2.16℃) in vertical temperature gradients. MERRA and NCEP1 also show warm SST biases at DJ, CB, and KM. However, in contrast to other products, relatively large wet biases in air humidity lead to relatively small biases in vertical humidity gradients (Fig. 5). Little or negative biases in wind speeds together with the reduced vertical humidity gradients contribute to small biases in LH fluxes for MERRA and NCEP1 at coastal sites DJ, CB, and KM. However, large underestimates of LH fluxes arise at offshore sites KJ, DH, and YS from dry biases and weak wind biases for MERRA and NCEP1. Hence, the small LH biases at coastal sites CB and KM for MERRA

and NCEP1 (Fig. 2, right) are not due to an accurate simulation of bulk variables in those products but due to the compensation of large errors in each variable that happens to make the variable combination agree better with the observation.

In the case of SH fluxes, only MERRAC show warm biases in air temperature over the whole region and in turn, similar or underestimated vertical temperature gradients to observations, leading large small biases (at DJ, CB and KM) and underestimates (at KJ DH and YS).

**3.2.2 Temporal characteristics of errors**

In Fig. 5 scatter plots of LH and SH fluxes at all sites derived from buoy observation and those from reanalysis products (recalculated ones) indicate that the systematic error of products caused by bulk variables depends on the magnitude of flux values. MERRAC and NCEP1C overestimate the fluxes for buoy observation values low, but they progressively underestimate the LH flux and SH flux for strong fluxes. This results in a cancellation of biases giving the appearance of a small overall bias. Other products show linear fit to buoy observation or slightly overestimate at high value. We showed all data in one scatterplot together, so individual feature at different location can be a little different, for example at most of products are underestimated for observation values high. It can be identified follow.

To examine time dependence of flux biases, seasonal variation of the biases for each product at six sites is illustrated in Figs. 7 and 8 together with the seasonal variation of LH and SH fluxes (black lines). The seasonal variation depicted in Figs. 7 and 8 is based on the average of all daily mean data values falling at a given date over the total record length. The seasonal variation of both LH and SH fluxes derived from buoy data is characterized by large amplitudes and high fluctuations in winter and vice versa in summer. This observed seasonal variation is due to strong winds and high vertical gradients of moisture and temperature in winter. The systematic error of products caused by variable biases tends to become larger in

winter, and the biases are dispersed amongst the products also in winter. NCEP1 and MERRA underestimate the turbulent heat fluxes in winter when the fluxes are large, and slightly overestimate the fluxes in summer when they are small (Fig 7). This results in a significant underestimation of total mean biases at DJ, KJ, DH, and YS, and a small overestimation at CB and KB. MERRA and NCEP1 have a similar mean bias pattern at each station when COARE3.0 algorithm is applied. However, the mean bias pattern of the original MERRA and NCEP1 is different (Fig. 2). NCEP1 overestimate turbulent heat flux in wintertime (at high heat flux period). These results indicate that magnitude and sign of total mean biases of reanalysis products are determined by error in winter.

**3.2.3 Sensitive test**

Sensitivity tests were performed to figure out which variable or combination of variables can reduce the mean bias of heat fluxes. Using the COARE 3.0 algorithm, a single variable or a pair of variables from the observation are replaced one by one with those in each of the reanalysis products and then mean biases for each product are estimated at all buoy sites (Figs. 9, 10, Table 13,14).

**a. Latent heat flux**

When the original biases of product with bulk variables from the product was already small (<10 $\mathrm{W}/m^2$), changes in the bias are insignificant (Figs. 9, 10, Table 13, 14), so we describe the sensitivity test results for the cases large original biases such as 1) large overestimates of fluxes for ERA-Interim, NCPE2, CFSR, and OAFlux at sites CB and KM, and 2) large underestimates of fluxes for MERRA and NCPE1 at sites KJ, DH, and YS.

At CB and KM, all combinations of observed bulk variables including SST remarkably reduce mean biases for ERA-Interim, NCPE2, CFSR, and OAFlux (Fig.9 and Table. 13). This is because accurate SST leads to improvement of the vertical gradient term. MERRA and NCEP1 had small biases with SST from the products at CB and KM, but they now largely

underestimate the fluxes with observed SST. This is because small biases of MERRA and NCEP1 with products' bulk variables resulted from the compensation effects of bulk variable biases. It then point out that the replacement of most biased variables with those observed ones does not guarantee the improvement result for all products. The errors in LH flux due to discrepancy in wind speed are also reduced by replacing with observed wind speeds, but not as much as the SST replacement. It indicates that the vertical temperature gradient is more important than the wind speed in improving the LH flux. The similar result was also found by Subrahamanyam et al. (2009) based on buoy data that the correlation between turbulent heat flux and vertical temperature gradient is better than that of turbulent heat flux and wind.

At KJ, DH, and YS, a combination of air humidity and wind speed reduces the mean biases of MERRA and NCPE1. This is a natural result because systematically wet bias of air specific humidity and weak wind caused underestimation in MERRA and NCPE1. However the change in vertical gradient terms (without wind) reduces the bias even more implying again that the vertical gradient term is more important than wind speed in reducing the biases.

**b. Sensible heat flux**

Magnitude of biases is small for all products, so any buoy variables reduced biases expect air temperature and air temperature and wind combination at CB and KM where warm air temperature rather reduces biases of vertical temperature gradients which are caused by large warm SST biases (Fig. 11, Table. 14).

Overall, the accurate vertical gradients term in the combination of variables can reduce the most bias of LH flux and SH flux, at all stations. On the other hands, the accurate SST in the single variables can improve the performance of products in many cases.

## 4. Summary

A common way to demine the quality of Numerical weather product is by comparison to different in-situ data. The meteorological variables gained from six flux buoys are used to calculate the latent and sensible heat flux with COARE3.0 algorithm and comparison of buoy-derived turbulent data with five reanalyzes products (ERA-Interim, NCEP1, NCEP2, CFSR, MERRA) and objectively analyzed data (OAflux) was conducted for validation over the East Asian Marginal Seas. Statistic tools were applied to figure out which products are closer to the value of buoy. Statistical analysis of bias and RMS difference of individual fields of LH flux and SH flux computation shows that most products are systematically overestimated in coastal regions. Especially, early NECP products significantly overestimate turbulent heat flux. This result is consistent with the previous studies at different region (Sun et al., 2003, Jiang et al., 2005, Kubota eat al 2009). Kubota pointed out that the overestimation of NCEP products is due largely to the bulk algorithm and is a general feature of the NCEP turbulent heat flux. While, MEERA have relatively lower values of turbulent heat flux compared to other products over the whole study domain. Roberts (2011) found that MERRA have systematically weak vertical gradients in moisture and temperature and in turn underestimate turbulent heat flux in Tropic Ocean. ERA- interim and CFSR are relatively accurate but they also show large biases for coastal region. Possible causes of errors for turbulent heat fluxes are mainly two: the bulk algorithm caused bias and input variable caused bias. Since turbulent heat fluxes from the buoy observation, which was used for reference here, are estimated using a bulk formula, they have also algorithm uncertainty. We focus on the variable-caused biases by calculating (or recalculating for some of reanalysis products) those fluxes using the same COARE 3.0 algorithm. Depending upon region and products, systematic overestimations are either reduced or remain similarly when the COARE algorithm is applied to recalculate the fluxes. MERRA and NCEP1 turned into

underestimation. ERA-interim, CFSR are not much changed (they still overestimate turbulent heat fluxes in coastal region). This indicates that ERA-Interim and CFSR algorithms behave similar to the COARE 3.0 algorithm. The biases of various input variable used to calculate turbulent heat flux are major cause for recalculated products. In this study, the overestimated heat losses in coastal region are caused mainly by the extremely warm biases of SST due to model's unsuitable parameterizations and coarse resolution to demonstrate regional ocean dynamic feature. Renfrew suggest (2002) recalculating flux with appropriate bulk algorithm and reanalysis bulk variable can reduce the disagreement in fluxes. Through the sensitive tests, it turned out that increasing the accuracy of both vertical temperature and humidity gradient, for LH flux and SH flux respectively, is the best ways to improve the performance of products. However it is difficult to obtain the high quality of humidity data in ocean for the data assimilation. While it is relatively easier to obtain high quality of sea surface temperature and it also gives good results in sensitive test. So we suggest that combination of COARE 3.0 algorithm and ERA-Interim or CFSR meteorological variables (which are least problematic variable over the study locations) and high resolution SST data, for example, from Group for High Resolution Sea Surface Temperature (GHRSST, 2011) could be reducing the flux difference.

# Reference


Bolton, D., 1980: The computation of equivalent potential temperature. *Mon. Wea. Rev.*, 108, 1046–1053.

Brunke, M. A., X. Zeng, and S. Anderson, 2002: Uncertainties in sea surface turbulent flux algorithms and data sets. *J. Geophys. Res.*, 107, 3141.

Brunke, M. A., C. W. Fairall, X. Zeng, L. Eymard, and J. A. Curry (2003), Which bulk aerodynamic algorithms are least problematic in computing ocean surface turbulent fluxes?, J. Clim., 16, 619–635.

Brunke, Michael A., Zhuo Wang, Xubin Zeng, Michael Bosilovich, Chung-Lin Shie, 2011: An Assessment of the Uncertainties in Ocean Surface Turbulent Fluxes in 11 Reanalysis, Satellite-Derived, and Combined Global Datasets. *J. Climate*, 24, 5469–5493.

Choi, H. Y., S. H. Lee, I. S. OH, 1998: Quantitative Analysis of Thermal Front in the Mid-eastern Coastal Area of the Yellow Sea. The Sea, Vol.3 No.1 1-8

Fairall, C. W., E. F. Bradley, G. A. Godfrey, G. A. Wick, J. B. Edson, and G. S. Young (1996a), Cool-skin and warm-layer effects on sea surface temperature, J. Geophys. Res., 101(C1), 1295– 1308.

Fairall, C. W., E. F. Bradley, D. P. Rogers, J. B. Edson, and G. S. Young (1996b), Bulk parameterization of air-sea fluxes for Tropical Ocean- Global Atmosphere Coupled-Ocean Atmosphere Response Experiment, J. Geophys. Res., 101(C2), 3747– 3764.

Fairall, C. W., E. F. Bradley, J. E. Hare, A. A. Grachev, and J. B. Edson (2003), Bulk parameterization of air-sea fluxes: Updates and verification for the COARE algorithm, J. Clim., 16, 571–591.

Gibson, J. K., P. Kallberg, A. Nomura, and S. Uppala, 1994: The ECMWF re-analysis (ERA) project- Plans and current status, 10th Int. Conf. on Interactive Information and

Processing Systems for Meteorology, Oceanography and Hydrology, Nashville, TN, Amer. Meteor. Soc., 164-167.

Hirose, N., Kim, C.H., Yoon, J.H., 1996. Head budget in the Japan Sea. Journal of Oceanography 52, 553–574.

Jiang, C.-L., M. F. Cronin, K. A. Kelly, and L. Thompson, 2005. Evaluation of a hybrid satellite and NWP based turbulent heat flux product using TAO buoys. J. Geophys. Res. 110, C09007, doi:10.1029/2004JC002824.

Kalnay, E., and Coauthors, 1996: The NCEP/NCAR 40-Year Reanalysis Project. *Bull. Amer. Meteor. Soc.*, 77, 437–471

Kanamitsu, M., W. Ebisuzaki, J. Woolen, J. Potter, and M. Fiorion, 2000: An overview of NCEP/DOE Reanalysis-2. *Proc. Second Int. Conf. on Reanalyses,* Reading, United Kingdom, WMO, 1–4.

Kubota, M., N. Iwabe, M. F. Cronin, and H. Tomita (2008), Surface heat fluxes from the NCEP/NCAR and NCEP/DOE reanalyses at the Kuroshio Extension Observatory buoy site, J. Geophys. Res., 113, C02009.

Liu, W. T., K. B. Katsaros, and J. A. Businger, 1979: Bulk parameterization of air–sea exchanges of heat and water vapor including the molecular constraints at the interface. *J. Atmos.*

*Sci.,* **36,** 1722–1735.

Moore, G. W. K., and I. A. Renfrew, 2002: An assessment of the surface turbulent heat fluxes from the NCEP-NCAR reanalysis over the western boundary currents, J. Climate, 15, 2020–2037.

Onogi, K., J. Tsutsui, H. Koide, M. Sakamoto, S. Kobayashi, H. Hatsushika, T. Matsumoto, N. Yamazaki, H. Kamahori, K. Takahashi, S. Kadokura, K. Wada, K. Kato, R. Oyama, T.

Ose, N. Mannoji, and R. Taira, 2007: The JRA-25 reanalysis. *J. Meteor. Soc. Japan*, **85**, 369-432.

Park, K., A. F., Sakaida, H., Kawamura, 2008: Error Characteristics of Satellite-observed sea surface temperature in the Northeast Asian Sea. Jour. Korean Earth Science Society, v.29 no3, p. 280-289.

Renfrew, Ian A., G. W. K. Moore, Peter S. Guest, and Karl Bumke, 2002: A Comparison of Surface Layer and Surface Turbulent Flux Observations over the Labrador Sea with ECMWF Analyses and NCEP Reanalyses. *J. Phys. Oceanogr.*, 32, 383–400.

Reynolds, R. W., and T. M. Smith, 1994: Improved global sea surface temperature analyses. *J. Climate*, 7, 929–948.

Roberts, J. Brent, Franklin R. Robertson, Carol A. Clayson, Michael G. Bosilovich, 2012: Characterization of Turbulent Latent and Sensible Heat Flux Exchange between the Atmosphere and Ocean in MERRA. *J. Climate*, 25, 821–838.

Saha, S., and Coauthors, 2010: The NCEP Climate Forecast System reanalysis. *Bull. Amer. Meteor. Soc.*, 91, 1015–1057

Subrahamanyam, D.B., Radhika, R., Rani, S.I., Kumar, B.P., 2007. Air–sea interaction processes over the East-Asian Marginal Seas surrounding the Korean Peninsula. Annales Geophysicae 25, 1477–1486.

Sun, B., L. Yu, and R. A. Weller (2003), Comparisons of surface meteorology and turbulent heat fluxes over the Atlantic: NWP model analyses versus moored buoy observations, J. Clim., 16, 679– 695.

Taylor, Peter K. (eds.) (2000) Intercomparison and validation of ocean–atmosphere energy flux fields. Final report of the Joint WCRP/SCOR Working Group on Air–Sea Fluxes (SCOR Working Group 110). Geneva, Switzerland, World Meteorological Organization,

World Climate Research Programme, 306pp. (WCRP Report, WCRP-112 (WMO/TD-1036))

Taylor, K.E.: Summarizing multiple aspects of model performance in a single diagram. *J. Geophys. Res.*, **106**, 7183-7192, 2001 (also see PCMDI Report 55, http://wwwpcmdi.llnl.gov/publications/ab55.html)

Trenberth, K. & Co-Authors (2010). "Atmospheric Reanalyses: A Major Resource for Ocean Product Development and Modeling" in *Proceedings of OceanObs'09: Sustained Ocean Observations and Information for Society (Vol. 2)*, Venice, Italy, 21-25 September 2009, Hall, J., Harrison, D.E. & Stammer, D., Eds., ESA Publication WPP-306, doi:10.5270/OceanObs09.cwp.90

Tomita, H., and M. Kubota,2006: An analysis of the accuracy of Japanese¥ Ocean Flux data sets with Use of Remote Sensing Observations (J-OFURO) satellite-derived latent heat flux using moored buoy data, J. Geophys. Res., 111, C07007, doi:10,1029/2005JC003013.

Uppala, S. M., and Coauthors, 2005: The ERA-40 Re-Analysis. *Quart. J. Roy. Meteor. Soc.*, 131, 2961–3012.

Weller, R. A., and S. P. Anderson, 1996: Surface meteorology and air–sea fluxes in the western equatorial Pacific warm pool during the TOGA Coupled Ocean–Atmosphere Response Experiment. *J. Climate,* **9,** 1959–1990.

Yu, Lisan, Robert A. Weller, Bomin Sun, 2004: Improving Latent and Sensible Heat Flux Estimates for the Atlantic Ocean (1988–99) by a Synthesis Approach*. J. Climate, 17, 373–393.

Yu, L., and R. A. Weller, 2007: Objectively analyzed air–sea heat fluxes for the global ice-free oceans (1981–2005). *Bull. Amer. Meteor. Soc.*, 88, 527–539.

Zeng, X., M. Zhao, and R. E. Dickinson, 1998: Intercomparison of bulk aerodynamic algorithms for the computation of sea surface fluxes using TOGA COARE and TAO data. *J. Climate*, 11, 2628–2644.

# Figure

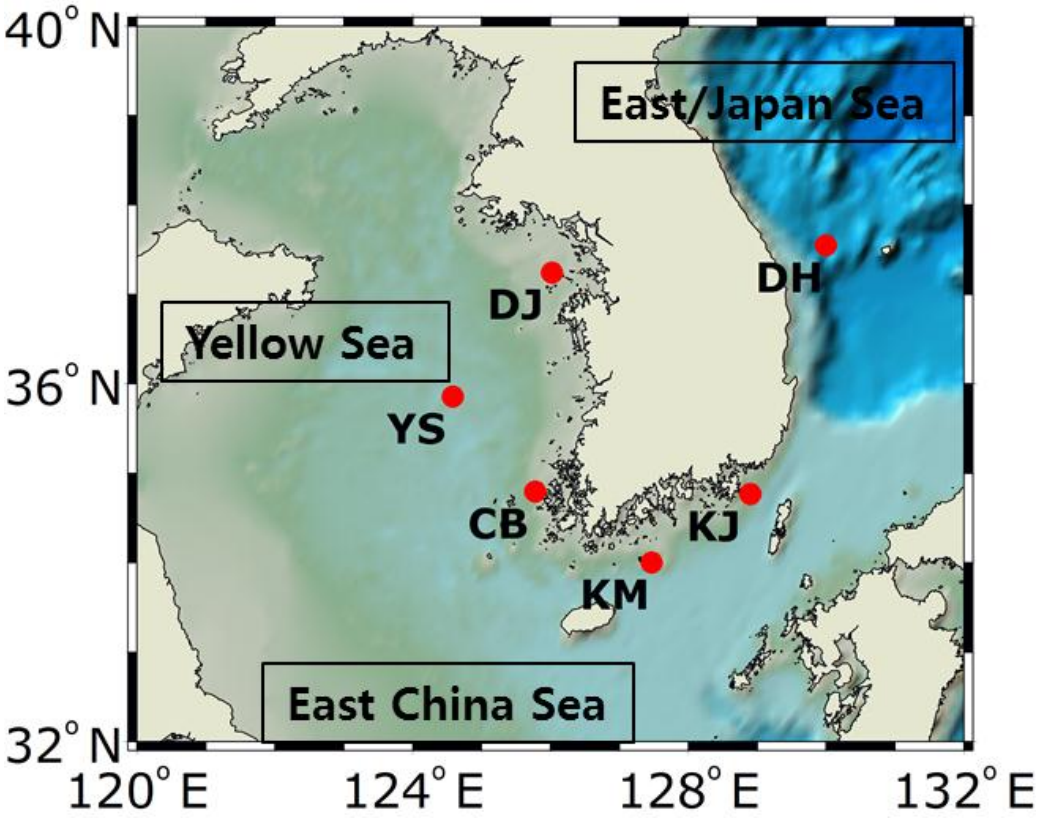


**Figure 1 Ocean buoy stations used for the flux inter-comparison**

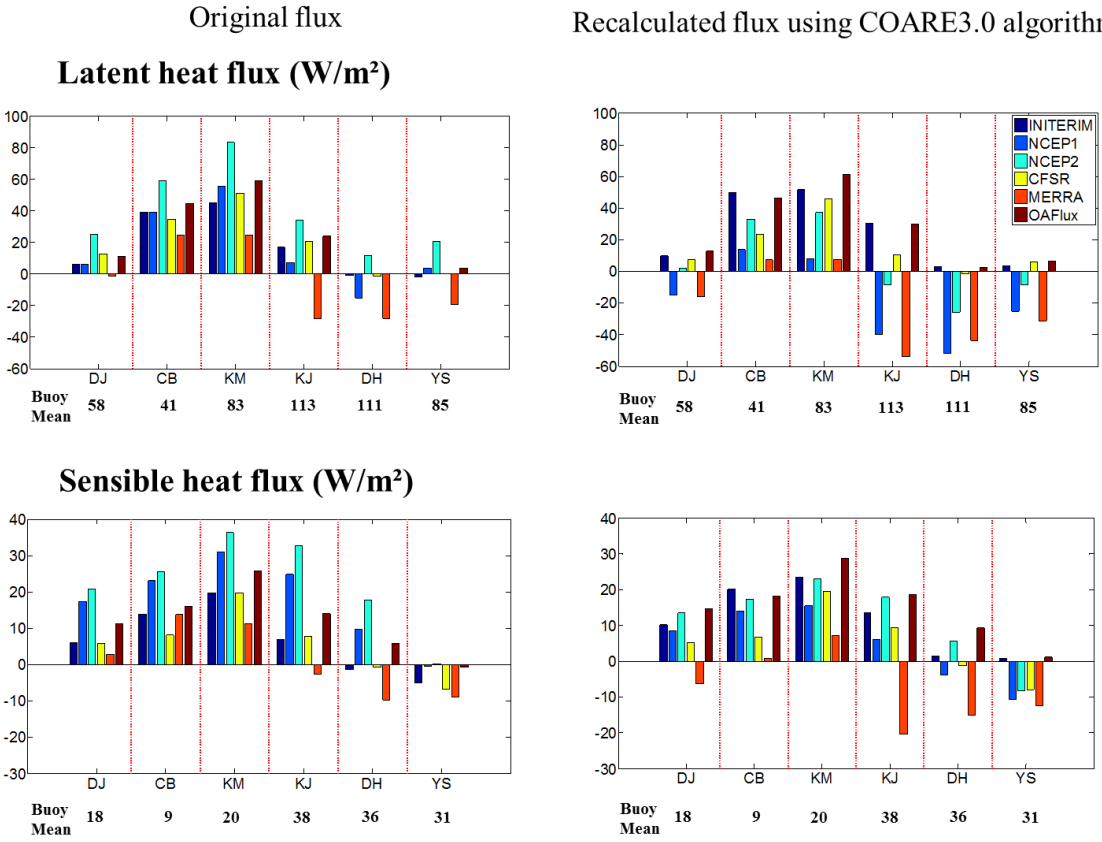


**Figure 2 Differences in latent and sensible heat fluxes ($\Delta Flux = Flux_{prod} - Flux_{buoys}$) at buoy stations. The left column shows the differences based on original fluxes with different bulk formulae and the right column based on the COARE algorithm. Record-length mean fluxes in W/m$^2$ at each buoy station (Buoy Mean) are shown in x-axis. Positive value in y-axis means the reanalysis products overestimate the fluxes (more heat loss) as compared to the fluxes based on the buoy observation.**

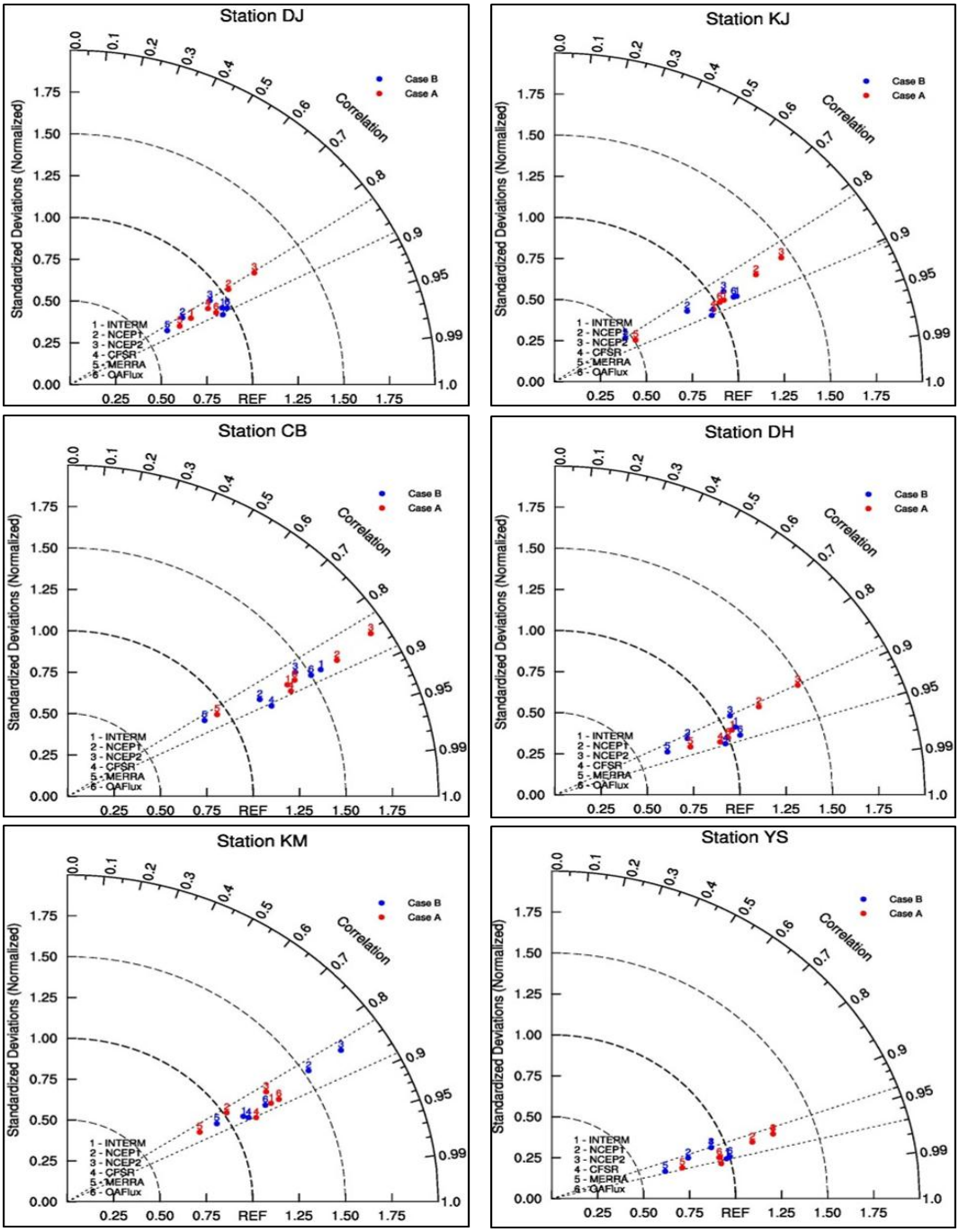


**Figure 3 Taylor diagrams of latent heat fluxes from six reanalysis products at six buoy sites. The radial co-ordinate gives the magnitude of total standard deviation, normalized by the observed value, and the angular co-ordinate gives the correlation with observations. The distance between the observed point (REF) and any product's point is proportional to the centered RMS error. All second-order statistics are calculated using the demeaned time series. (Case A = original fluxes, Case B= Recalculated fluxes using COARE 3.0 algorithm).**

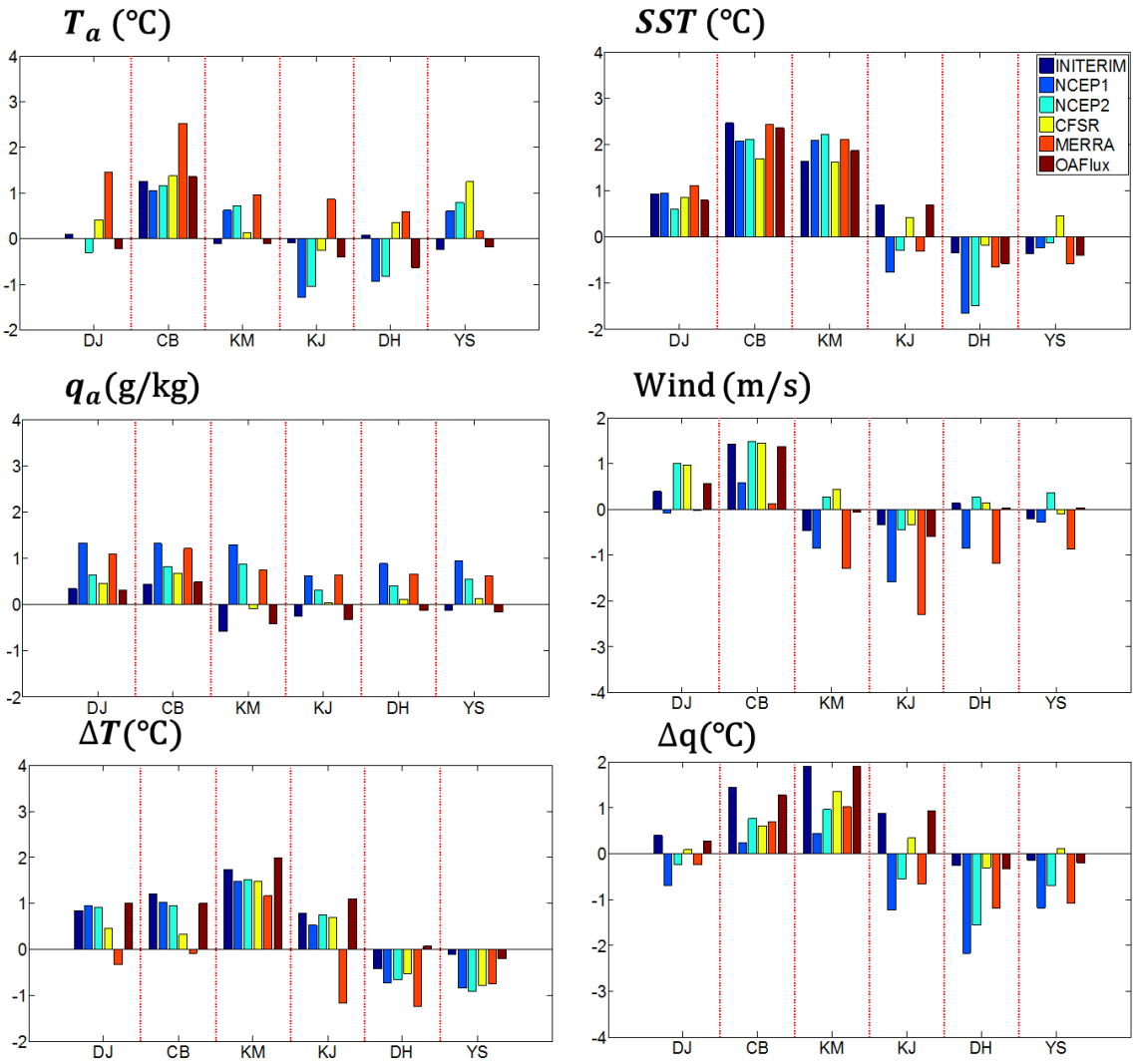


**Figure 4 Differences in variables used for the flux calculation between those measured by buoys and derived from products. Ta: air temperature at 2 m, SST: sea surface temperature qa: specific humidity, air at 2 m, qs: specific humidity at sea surface, Wind: wind speed at 10 m, ΔT: temperature gradient (Ta – SST), Δq: specific humidity gradient (qa – qs).**

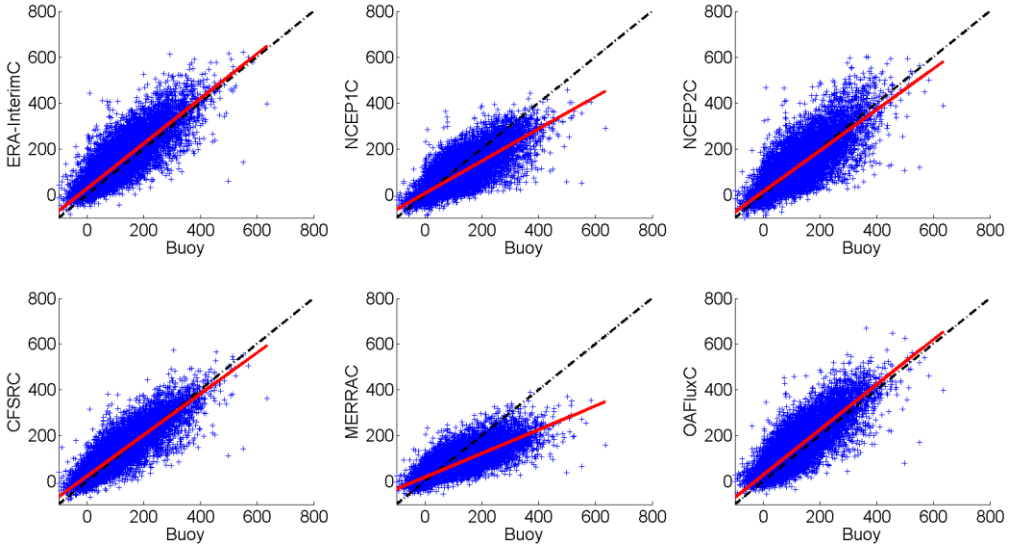


**Figure 5 Scatter plots of daily mean latent heat fluxes ($W/m^2$) derived from all buoy observations (x-axis) and from each reanalysis product (y-axis). Linear regression line ( red) and the 1 to 1 line (black) are shown.**

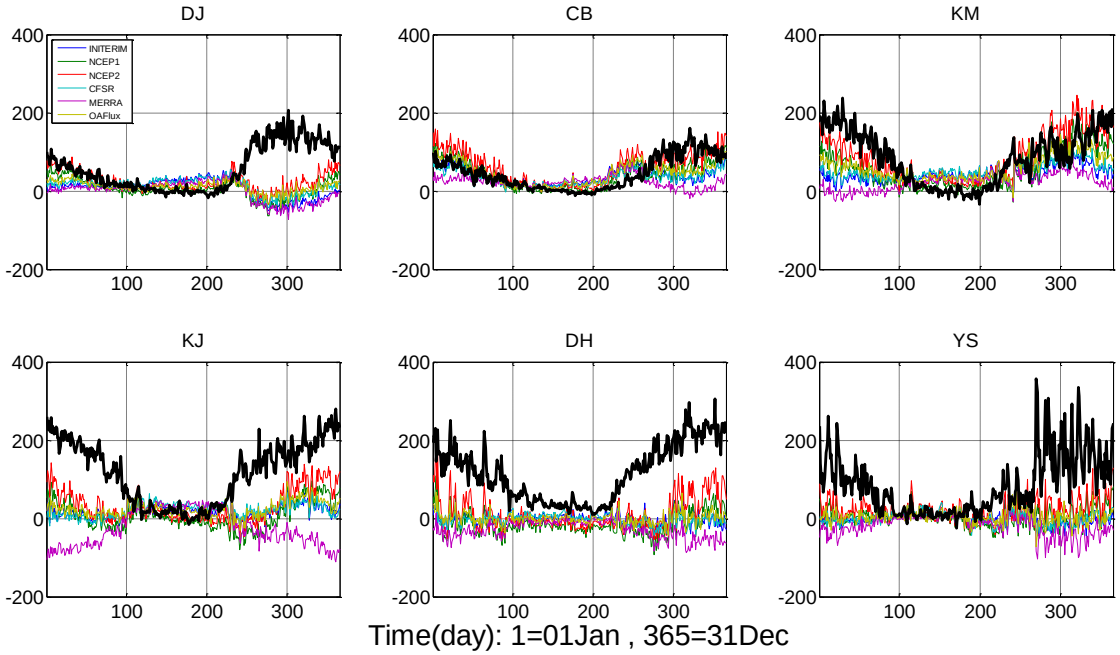


**Figure 6 Seasonal variation of latent heat flux ($W/m^2$) based on buoy observation (thick black line), and mean differences of product's latent heat flux with observation (colors). Positive (negative) values of the difference denote the latent flux from the product overestimates (underestimates) the flux.**

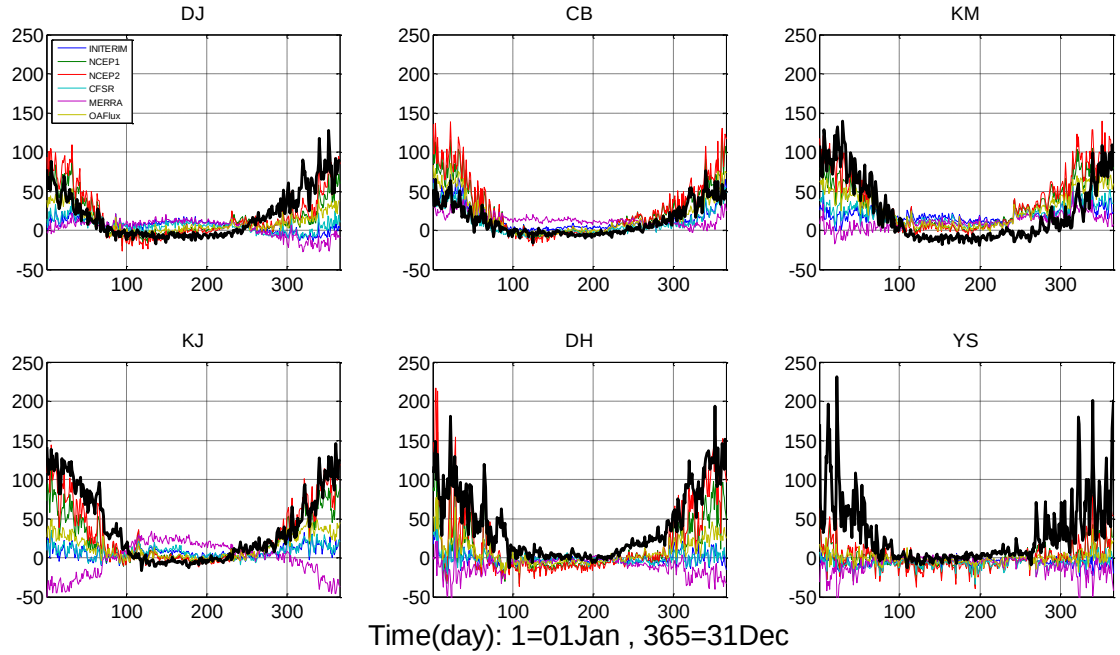


**Figure 7 Same as Fig. 6 for sensible heat flux ($W/m^2$).**

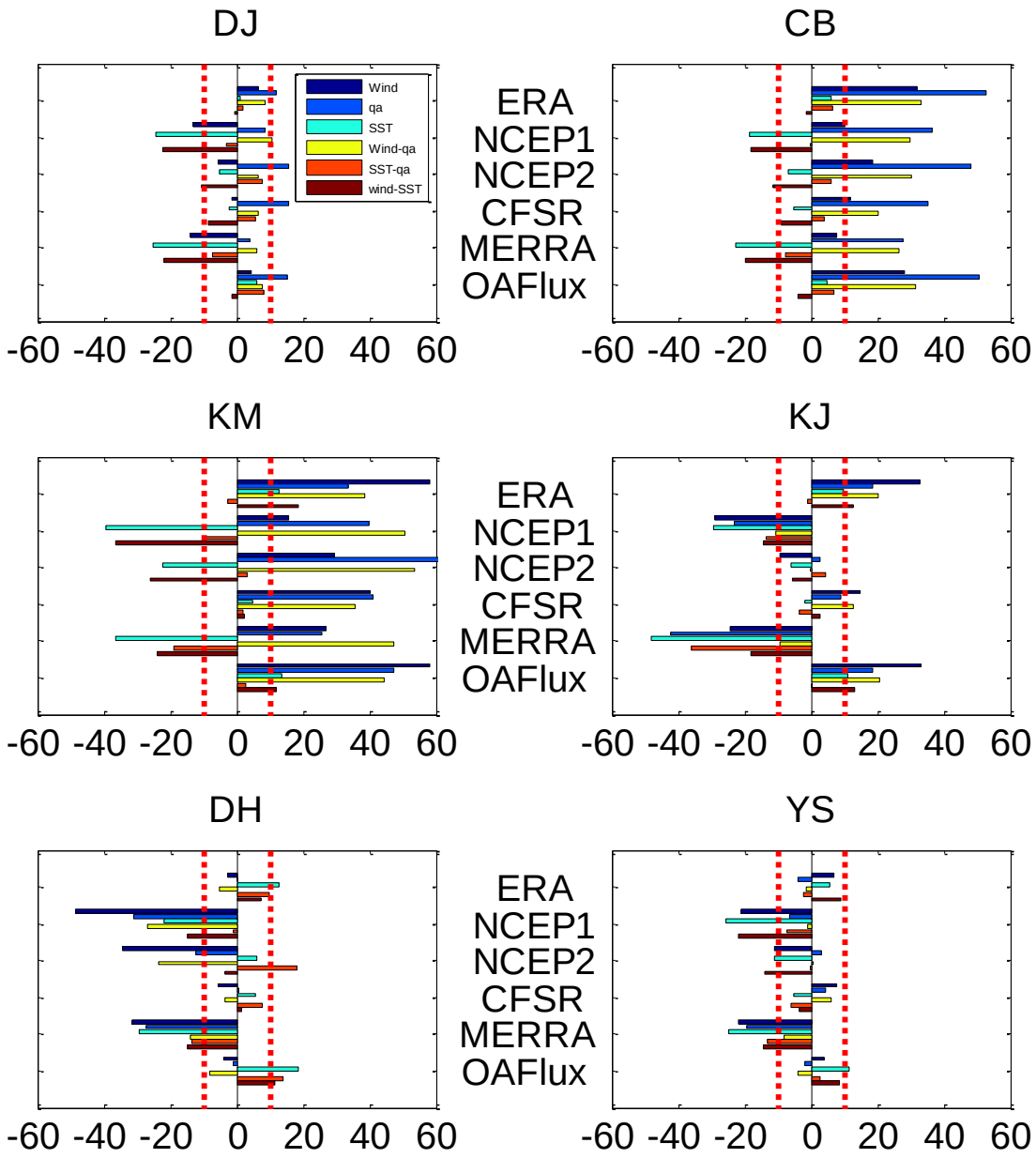


**Figure 8 Sensitive test of various combinations (Wind, SST, $q_a$, wind-$q_a$, SST-$q_a$ wind-SST) of these variables to figure out which variable or combination of variables can reduce the latent heat flux difference (W/$m^2$).**

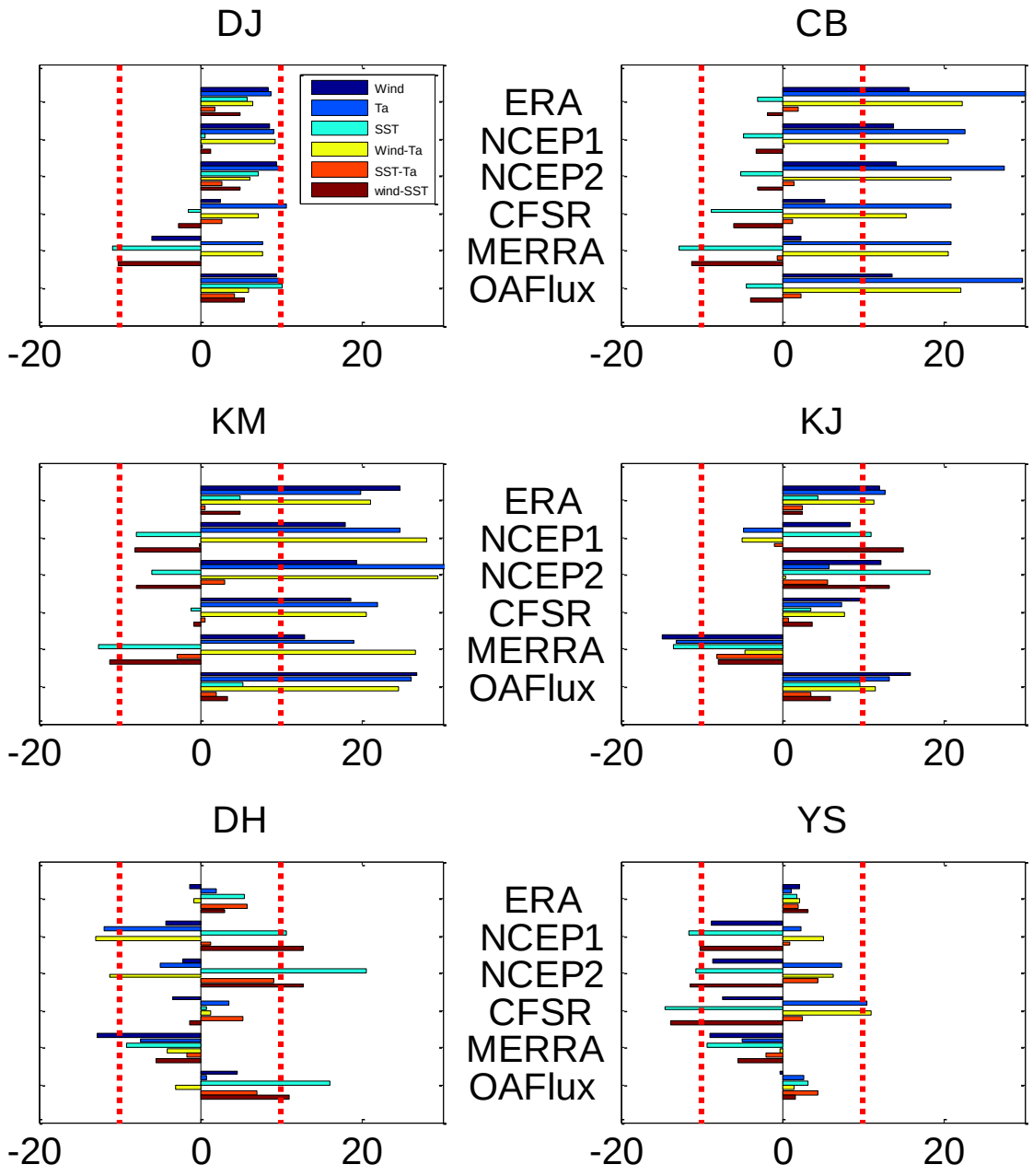


**Figure 9 Sensitive test of various combinations (Wind, SST, $T_a$, wind-$T_a$, SST-$T_a$, wind SST) of these variables to figure out which variable or combination of variables can reduce the sensible flux difference ($W/m^2$).**

# Table

**Table 1 Periods of available buoy data at each buoy site and Number of daily mean observations during 1997-2009. Dates longer than 300 days are highlighted in red.**

| Year /Station | 1997 | 1998 | 1999 | 2000 | 2001 | 2002 | 2003 | 2004 | 2005 | 2006 | 2007 | 2008 | 2009 |
|---|---|---|---|---|---|---|---|---|---|---|---|---|---|
| DJ | 91 | - | 316 | 218 | 236 | 338 | 248 | 275 | 316 | 351 | 342 | 318 | 324 |
| | 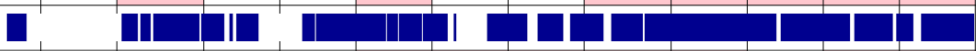 | | | | | | | | | | | | |
| CB | 19 | 160 | 154 | 221 | 185 | 346 | 343 | 337 | 303 | 344 | 243 | 366 | 326 |
| | 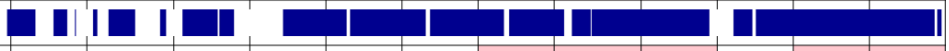 | | | | | | | | | | | | |
| KM | - | 188 | 244 | 253 | 236 | 242 | 103 | 315 | 322 | 318 | 238 | 323 | 365 |
| |  | | | | | | | | | | | | |
| KJ | - | 218 | 254 | 200 | 332 | 294 | 291 | 341 | 322 | 298 | 365 | 346 | 351 |
| |  | | | | | | | | | | | | |
| DH | - | - | - | - | 212 | 365 | 206 | 158 | 124 | 311 | 169 | 235 | 331 |
| |  | | | | | | | | | | | | |
| YS | - | - | - | - | - | - | - | - | - | - | 109 | 357 | 237 |
| |  | | | | | | | | | | | | |

**Table 2 Information of buoys and buoy observation.**

| Station | Depth(m) | Distance from land(km) | Sensor height(m) (Wind/Ta/Rh) | Period |
|---|---|---|---|---|
| DJ | 30 | 5.8 | 4.8/3.8/3.8 | 1997~2009 |
| CB | 33 | 10.8 | 4.8/3.8/3.8 | 1998~2009 |
| KM | 80 | 44.4 | 4.8/3.8/3.8 | 1998~2009 |
| KJ | 84 | 17 | 4.8/3.8/3.8 | 1998~2009 |
| DH | 1518 | 66.8 | 3.8/3.3/3.3 | 2001~2009 |
| YS | 90 | 177 | 10/10/10 | 2007~2009 |

**Table 3 Analyzed reanalysis products.**

| Name | Resolution | Period | Type | Feature |
|---|---|---|---|---|
| NCEP/NCAR (NCEP1) | 1.875°x1.875° | 1948-present | Reanalyses | 3D-var |
| NCEP-DOE (NCEP2) | 1.875°x1.875° | 1979-present | Reanalyses | 3D-var<br>Revised version of NECP1 |
| NCEP-CFSR (CFSR) | 0.5°x0.5° | 1979- 2009 | Reanalyses | 3D-var<br>Atmosphere-ocean coupled model |
| ERA-Interim | 1.5°x1.5° | 1989-present | Reanalyses | 4D-var |
| MERRA | 1/2°x2/3° | 1979-present | Reanalyses | 3D-var<br>GEOS-5 |
| OAFlux | 1°x1° | 1989-present | Blended | OA mapping<br>(Reanlyses+satellite) +in-situ) |

**Table 4 Error analysis in the calculation of latent and sensible heat fluxes using observed bulk sea surface temperature at buoy sites rather than using the skin temperature as in the reanalysis products.**

| #/bias | Latent | Sensible |
|---|---|---|
| DJ | 2.32 | 1.31 |
| CB | 2.24 | 1.26 |
| KJ | 3.82 | 1.87 |
| KM | 4.40 | 2.07 |
| DH | 3.95 | 1.94 |
| YS | 3.37 | 1.83 |

**Table 5 Results of RECALD minus ORID for the latent heat flux from the six reanalysis products at six buoy sites. See the text for the definition of ORDI and RECALD.**

| Buoy/Products | ERA-Interim | NCEP1 | NCEP2 | CFSR | MERRA | OAFlux |
|---|---|---|---|---|---|---|
| DJ | 3.8 | -21.2 | -22.8 | -5.6 | -14.5 | 1.7 |
| CB | 10.4 | -25.6 | -26.3 | -11.5 | -17.4 | 1.5 |
| KM | 6.7 | -47.4 | -46.2 | -5.5 | -17.3 | 2.2 |
| KJ | 13.4 | -47.3 | -42.4 | -10.3 | -25.8 | 5.7 |
| DH | 3.7 | -36.9 | -37.2 | -0.2 | -15.8 | 2.5 |
| YS | 5.3 | -29.2 | -28.9 | 5.89 | -12.0 | 2.5 |

**Table 6 Same as Table 4 for sensible heat flux**

| Buoy/Products | ERA-Interim | NCEP1 | NCEP2 | CFSR | MERRA | OAFlux |
|---|---|---|---|---|---|---|
| DJ | 4.2 | -8.9 | -7.2 | -0.7 | -9.1 | 3.2 |
| CB | 6.3 | -9.0 | -8.3 | -1.5 | -12.9 | 2.2 |
| KM | 3.7 | -15.5 | -13.1 | -0.2 | -4.1 | 3.0 |
| KJ | 6.6 | -18.7 | -14.8 | 1.6 | -17.8 | 4.5 |
| DH | 2.8 | -13.7 | -12.0 | -0.5 | -5.4 | 3.6 |
| YS | 5.9 | -10.1 | -8.6 | -1.1 | -3.6 | 1.9 |

**Table 7 . Record-length mean latent (R_LH) and sensible (R_SH) heat fluxes, SST, air temperature ($T_a$), air humidity ($Q_a$), air–sea temperature difference ($SST$- $T_a$), air–sea humidity difference ($Q_s$-$Q_a$), and 10-m wind speed at each buoy site (second row in the Table), and their differences for each product with the observation together with ±1 standard deviation of the difference.**

| Source | R_LH ($Wm^{-2}$) | R_SH ($Wm^{-2}$) | SST(℃) | Ta(℃) | Qa(g/kg) | SST-Ta(℃) | Qs-Qa (g/kg) | Wind(m/s) |
|---|---|---|---|---|---|---|---|---|
| Buoy | 61.7 | 19.9 | 13.35 | 7.73 | 7.73 | 0.97 | 2.43 | 4.56 |
| Interim-Buoy | 9.9±37.7 | 10.1±25.2 | 1.12±1.74 | 0.11±2.39 | 0.34±1.41 | 1.01±1.97 | 0.52±1.82 | 0.40±1.18 |
| NCEP1-Buoy | -14.8±42.9 | 8.4±23.9 | 1.14±1.51 | 0.02±1.77 | 1.33±1.54 | 1.12±1.91 | -0.58±1.83 | -0.08±1.54 |
| NCEP2-Buoy | 2.2±42.8 | 13.6±33.3 | 0.78±1.51 | -0.30±1.89 | 0.63±1.53 | 1.08±2.01 | -0.12±1.85 | 1.01±1.85 |
| CFSR-Buoy | 7.3±34.6 | 5.2±22.0 | 1.04±1.23 | 0.42±1.63 | 0.47±1.37 | 0.63±1.68 | 0.21±1.71 | 0.97±1.12 |
| MERRA-Buoy | -15.9±43.9 | -6.320.5 | 1.30±1.74 | 1.47±1.71 | 1.09±1.48 | -0.17±1.87 | -0.11±2.10 | -0.02±1.39 |
| OAFLux-Buoy | 12.9±36.9 | 14.6±26.7 | 0.98±1.36 | -0.20±2.04 | 0.30±1.47 | 1.18±1.81 | 0.39±1.75 | 0.56±1.32 |

**Table 8 Same as Table 7 but for CB**

| Source | R_LH ($Wm^{-2}$) | R_SH ($Wm^{-2}$) | SST(℃) | Ta(℃) | Qa(g/kg) | SST-Ta(℃) | Qs-Qa (g/kg) | Wind(m/s) |
|---|---|---|---|---|---|---|---|---|
| Buoy | 43.7 | 11.0 | 14.36 | 8.72 | 8.72 | 0.57 | 1.80 | 4.50 |
| Interim-Buoy | 49.9±48.3 | 20.1±34.7 | 2.65±1.64 | 1.27±2.05 | 0.44±1.36 | 1.38±2.07 | 1.58±1.47 | 1.43±1.28 |
| NCEP1-Buoy | 13.6±33.4 | 14.0±25.7 | 2.26±1.67 | 1.07±1.70 | 1.32±1.46 | 1.20±1.89 | 0.37±1.37 | 0.58±1.75 |
| NCEP2-Buoy | 32.7±44.6 | 17.4±34.1 | 2.30±1.65 | 1.17±1.78 | 0.83±1.41 | 1.13± 2.02 | 0.89±1.38 | 1.48±2.04 |
| CFSR-Buoy | 23.2±31.6 | 6.7±20.9 | 1.88±1.51 | 1.39±1.62 | 0.68±1.30 | 0.49±1.38 | 0.73±1.22 | 1.46±1.30 |
| MERRA-Buoy | 7.4±30.1 | 0.8±13.9 | 2.63±1.62 | 2.54±1.74 | 1.21±1.48 | 0.08±1.44 | 0.83±1.53 | 0.13±1.52 |
| OAFLux-Buoy | 46.3±45.3 | 18.2±31.8 | 2.55±1.56 | 1.37±1.79 | 0.49±1.39 | 1.17±1.88 | 1.40±1.39 | 1.38±1.37 |

**Table 9 Same as Table 7 but for KJ**

| Source | R_LH ($Wm^{-2}$) | R_SH ($Wm^{-2}$) | SST(℃) | Ta(℃) | Qa(g/kg) | SST-Ta(℃) | Qs-Qa (g/kg) | Wind(m/s) |
|---|---|---|---|---|---|---|---|---|
| Buoy | 80.2 | 20.0 | 17.40 | 10.07 | 10.07 | 0.85 | 2.49 | 6.61 |
| Interim-Buoy | 51.7±56.1 | 23.5±31.2 | 1.82±1.48 | -0.09±1.63 | -0.57±1.15 | 1.91±2.19 | 2.04±1.63 | -0.47±1.53 |
| NCEP1-Buoy | 8.3±51.8 | 15.5±23.4 | 2.28±1.82 | 0.63±1.08 | 1.29±1.32 | 1.65±1.75 | 0.59±1.68 | -0.85±2.23 |
| NCEP2-Buoy | 37.2±62.2 | 23.2±33.0 | 2.41±1.80 | 0.73±1.03 | 0.88±1.35 | 1.68±1.86 | 1.11±1.70 | 0.28±2.43 |
| CFSR-Buoy | 45.8±47.4 | 19.5±24.4 | 1.79±1.41 | 0.14±0.95 | -0.09±1.08 | 1.66±1.51 | 1.51±1.47 | 0.43±1.28 |
| MERRA-Buoy | 7.6±47.3 | 7.2±20.1 | 2.30±1.61 | 0.97±0.97 | 0.75±1.25 | 1.34±1.50 | 1.17±1.67 | -1.30±1.86 |
| OAFLux-Buoy | 61.3±59.1 | 28.9±33.3 | 2.06±1.49 | -0.11±1.28 | -0.42±1.22 | 2.16±2.00 | 2.05±1.60 | -0.07±1.76 |

**Table 10 Same as Table 7 but for KM**

| Source | R_LH ($Wm^{-2}$) | R_SH ($Wm^{-2}$) | SST(℃) | Ta(℃) | Qa(g/kg) | SST-Ta(℃) | Qs-Qa (g/kg) | Wind(m/s) |
|---|---|---|---|---|---|---|---|---|
| Buoy | 124.8 | 40.2 | 18.37 | 9.16 | 9.16 | 2.67 | 4.08 | 6.82 |
| Interim-Buoy | 30.3±55.7 | 13.6±31.3 | 0.89±1.55 | -0.07±1.71 | -0.26±0.90 | 0.96±1.84 | 1.04±1.45 | -0.34±1.74 |
| NCEP1-Buoy | -40.1±54.9 | 6.1±28.2 | -0.57±1.70 | -1.27±0.40 | 0.61±1.17 | 0.70±1.77 | -1.08±1.48 | -1.59±2.30 |
| NCEP2-Buoy | -8.4±59.5 | 17.9±42.2 | -0.11±1.69 | -1.04±1.58 | 0.31±1.17 | 0.93±1.98 | -0.40±1.50 | -0.44±2.59 |
| CFSR-Buoy | 10.6±45.9 | 9.4±25.3 | 0.62±1.46 | -0.25±1.41 | 0.04±0.92 | 0.86±1.57 | 0.50±1.37 | -0.33±1.47 |
| MERRA-Buoy | -54.1±71.9 | -20.4±32.2 | -0.13±2.24 | 0.87±1.46 | 0.64±1.20 | -1.00±1.72 | -0.50±2.29 | -2.30±1.90 |
| OAFLux-Buoy | 29.8±55.3 | 18.6±31.6 | 0.88±1.50 | -0.39±1.67 | -0.33±1.04 | 1.27±1.85 | 1.08±1.47 | -0.59±1.98 |

**Table 11 Same as Table 7 but for DH**

| Source | R_LH ($Wm^{-2}$) | R_SH ($Wm^{-2}$) | SST(℃) | Ta(℃) | Qa(g/kg) | SST-Ta(℃) | Qs-Qa (g/kg) | Wind(m/s) |
|---|---|---|---|---|---|---|---|---|
| Buoy | 112.7 | 36.6 | 17.88 | 8.74 | 8.74 | 2.68 | 4.16 | 5.94 |
| Interim-Buoy | 30.3±40.0 | 1.4±22.4 | -0.35±1.27 | 0.09±1.37 | -0.00±0.68 | -0.25±1.48 | -0.11±1.19 | 0.14±1.46 |
| NCEP1-Buoy | -40.1±42.9 | -3.9±21.8 | -1.66±1.31 | -0.93±1.33 | 0.89±1.04 | -0.55±1.48 | -2.02±1.30 | -0.84±2.09 |
| NCEP2-Buoy | -8.4±46.6 | 5.6±41.2 | -1.49±1.31 | -0.82±1.52 | 0.41±1.04 | -0.48±1.74 | -1.40±1.25 | 0.26±2.58 |
| CFSR-Buoy | 10.6±31.0 | -1.3±17.0 | -1.18±0.99 | 0.36±0.95 | 0.11±0.68 | -0.35±1.06 | -0.15±1.01 | 0.14±1.11 |
| MERRA-Buoy | -54.1±45.5 | -15.1±19.9 | -0.66±1.20 | 0.60±1.08 | 0.66±1.03 | -1.07±1.09 | -1.03±1.34 | -1.17±1.58 |
| OAFLux-Buoy | 29.8±35.1 | 9.3±24.9 | -0.57±1.08 | -0.63±1.42 | -0.12±0.87 | 0.24±1.42 | -0.19±1.12 | 0.03±1.43 |

**Table 4 Same as Table 7 but YS**

| Source | R_LH ($Wm^{-2}$) | R_SH ($Wm^{-2}$) | SST(℃) | Ta(℃) | Qa(g/kg) | SST-Ta(℃) | Qs-Qa (g/kg) | Wind |
|---|---|---|---|---|---|---|---|---|
| Buoy | 84.4 | 30.6 | 15.37 | 8.16 | 8.16 | 2.04 | 3.28 | 5.93 |
| Interim-Buoy | 3.5±21.4 | 0.9±11.0 | -0.36±2.51 | -0.22±1.13 | -0.12±0.70 | -0.12±2.86 | -0.14±1.73 | -0.21±2.55 |
| NCEP1-Buoy | -25.3±30.9 | -10.6±14.8 | -0.23±2.36 | 0.63±0.92 | 0.94±1.06 | -0.84±0.1 | -1.18±2.18 | -0.28±2.56 |
| NCEP2-Buoy | -8.3±29.2 | -8.3±13.9 | 0.12±2.35 | 0.82±0.91 | 0.54±1.12 | -0.90±2.06 | -0.70±1.99 | 0.36±2.79 |
| CFSR-Buoy | 6.2±22.7 | -7.9±8.3 | 0.46±0.91 | 1.25±0.85 | 0.12±0.76 | -0.78±0.61 | 0.11±1.04 | -0.09±0.97 |
| MERRA-Buoy | -31.3±36.0 | -12.5±17.3 | -0.58±2.51 | 0.20±0.69 | 0.62±0.95 | -0.75±2.27 | -1.1±1.90 | -0.87±2.56 |
| OAFLux-Buoy | 6.3±22.2 | 1.2±10.6 | -0.40±2.62 | -0.17±0.92 | -0.16±0.83 | -0.21±2.77 | -0.2±1.84 | 0.04±2.34 |

**Table 5 Results of sensitive test for LH flux ($W/m^2$). Red shading indicates mean biases less than 10 $W/m^2$ and Original bias at each site.**

| Station | Products | Wind | qa | SST | qa/Wind | qa/qs | Wind/as | Original |
|---|---|---|---|---|---|---|---|---|
| DJ (57.88) | INTERIM | 6.54 | 11.76 | 0.88 | 8.55 | 2.02 | -0.43 | 12.24 |
| | NCEP1 | -13.29 | 8.63 | -24.47 | 10.77 | -2.97 | -22.42 | -12.52 |
| | NCEP2 | -5.65 | 15.43 | -5.27 | 6.33 | 7.53 | -10.63 | 4.04 |
| | CFSR | -1.27 | 15.52 | -2.32 | 6.45 | 5.67 | -8.40 | 9.46 |
| | MERRA | -13.99 | 3.84 | -25.17 | 6.10 | -7.21 | -21.95 | -13.25 |
| | OAFlux | 4.54 | 15.07 | 6.02 | 7.50 | 7.97 | -1.66 | 14.87 |

| Station | Products | Wind | qa | SST | qa/Wind | qa/qs | Wind/as | Original |
|---|---|---|---|---|---|---|---|---|
| CB (41.36) | INTERIM | 31.83 | 52.53 | 6.22 | 33.19 | 6.59 | -1.44 | 50.28 |
| | NCEP1 | 10.26 | 36.60 | -18.38 | 29.97 | -0.35 | -18.08 | 13.99 |
| | NCEP2 | 18.48 | 48.06 | -6.76 | 30.18 | 5.94 | -11.56 | 33.14 |
| | CFSR | 11.80 | 35.11 | -5.07 | 20.01 | 4.09 | -8.87 | 23.78 |
| | MERRA | 7.80 | 27.71 | -22.64 | 26.66 | -7.88 | -19.65 | 7.75 |
| | OAFlux | 28.11 | 50.77 | 4.80 | 31.31 | 6.94 | -3.88 | 46.75 |

| Station | Products | Wind | qa | SST | qa/Wind | qa/qs | Wind/as | Original |
|---|---|---|---|---|---|---|---|---|
| KM (82.90) | INTERIM | 58.31 | 33.47 | 12.68 | 38.65 | -2.91 | 18.56 | 52.79 |
| | NCEP1 | 15.48 | 39.73 | -39.21 | 50.76 | -9.69 | -36.38 | 9.38 |
| | NCEP2 | 29.36 | 62.53 | -22.46 | 53.54 | 3.01 | -26.06 | 38.32 |
| | CFSR | 40.09 | 40.88 | 4.63 | 35.73 | 1.70 | 2.43 | 47.07 |
| | MERRA | 26.77 | 25.54 | -36.44 | 47.43 | -18.98 | -23.92 | 8.79 |
| | OAFlux | 58.06 | 47.36 | 13.74 | 44.55 | 2.52 | 12.01 | 62.39 |

| Station | Products | Wind | qa | SST | qa/Wind | qa/qs | Wind/as | Original |
|---|---|---|---|---|---|---|---|---|
| KJ (112.85) | INTERIM | 32.88 | 18.55 | 9.95 | 20.17 | -1.08 | 12.53 | 31.50 |
| | NCEP1 | -28.76 | -23.17 | -29.29 | -10.55 | -13.39 | -14.19 | -38.87 |
| | NCEP2 | -9.38 | 2.70 | -5.89 | -0.12 | 4.33 | -5.80 | -7.14 |
| | CFSR | 14.89 | 8.78 | -1.77 | 12.63 | -3.38 | 2.60 | 11.97 |
| | MERRA | -24.40 | -42.25 | -47.97 | -9.38 | -35.98 | -17.97 | -52.82 |
| | OAFlux | 33.27 | 18.34 | 10.93 | 20.57 | 0.17 | 13.31 | 30.97 |

| Station | Products | Wind | qa | SST | qa/Wind | qa/qs | Wind/as | Original |
|---|---|---|---|---|---|---|---|---|
| DH (110.91) | INTERIM | -2.52 | 0.39 | 12.79 | -5.40 | 9.93 | 7.40 | 7.17 |
| | NCEP1 | -48.62 | -30.88 | -22.00 | -26.68 | -1.05 | -14.86 | -47.56 |
| | NCEP2 | -34.37 | -12.39 | 6.16 | -23.36 | 18.22 | -3.37 | -21.45 |
| | CFSR | -5.46 | 0.54 | 5.82 | -3.61 | 7.54 | 1.61 | 3.44 |
| | MERRA | -31.46 | -27.47 | -29.37 | -13.80 | -13.59 | -14.94 | -39.27 |
| | OAFlux | -3.77 | -1.17 | 18.42 | -8.32 | 13.80 | 11.39 | 7.07 |

| Station | Products | Wind | qa | SST | qa/Wind | qa/qs | Wind/as | Original |
|---|---|---|---|---|---|---|---|---|
| YB (84.59) | INTERIM | 6.83 | -4.10 | 5.53 | -1.31 | -2.35 | 8.82 | 3.41 |
| | NCEP1 | -20.90 | -6.59 | -25.47 | -1.09 | -7.30 | -22.02 | -25.45 |
| | NCEP2 | -10.92 | 2.94 | -10.86 | 0.61 | -0.25 | -13.98 | -8.47 |
| | CFSR | 7.83 | 4.40 | -5.16 | 6.03 | -6.21 | -3.39 | 6.20 |
| | MERRA | -21.71 | -19.40 | -24.64 | -8.26 | -13.18 | -14.18 | -31.51 |
| | OAFlux | 3.91 | -1.72 | 11.28 | -4.06 | 2.76 | 8.65 | 6.16 |

**Table 14 Results of sensitive test for SH flux ($W/m^2$). Red shading indicates mean biases less than 10 $W/m^2$ and Original bias at each site.**

| Station | Products | Wind | Ta | SST | Ta/Wind | Ta/SST | Wind/SST | Original |
|---|---|---|---|---|---|---|---|---|
| DJ (17.74) | INTERIM | 8.39 | 8.70 | 5.86 | 6.39 | 1.76 | 4.97 | 11.46 |
| | NCEP1 | 8.56 | 9.06 | 0.62 | 9.17 | 0.22 | 1.19 | 9.65 |
| | NCEP2 | 9.48 | 9.86 | 7.14 | 6.20 | 2.58 | 4.88 | 14.61 |
| | CFSR | 2.48 | 10.64 | -1.51 | 7.14 | 2.59 | -2.65 | 6.57 |
| | MERRA | -6.06 | 7.75 | -10.92 | 7.61 | 0.06 | -10.19 | -4.56 |
| | OAFlux | 9.45 | 9.84 | 10.17 | 6.00 | 4.19 | 5.48 | 15.72 |

| Station | Products | Wind | Ta | SST | Ta/Wind | Ta/SST | Wind/SST | Original |
|---|---|---|---|---|---|---|---|---|
| CB (9.02) | INTERIM | 15.76 | 30.09 | -3.03 | 22.35 | 1.89 | -1.85 | 20.80 |
| | NCEP1 | 13.70 | 22.59 | -4.76 | 20.56 | 0.25 | -3.25 | 14.71 |
| | NCEP2 | 14.04 | 27.50 | -5.09 | 20.92 | 1.42 | -3.11 | 18.07 |
| | CFSR | 5.28 | 20.85 | -8.82 | 15.39 | 1.22 | -6.04 | 7.47 |
| | MERRA | 2.27 | 20.93 | -12.81 | 20.60 | -0.69 | -11.17 | 1.46 |
| | OAFlux | 13.61 | 29.78 | -4.44 | 22.05 | 2.35 | -3.88 | 18.84 |

| Station | Products | Wind | Ta | SST | Ta/Wind | Ta/SST | Wind/SST | Original |
|---|---|---|---|---|---|---|---|---|
| KM (20.33) | INTERIM | 24.71 | 19.79 | 4.87 | 21.04 | 0.50 | 4.93 | 24.95 |
| | NCEP1 | 17.91 | 24.70 | -7.90 | 27.95 | -0.06 | -8.15 | 17.01 |
| | NCEP2 | 19.35 | 33.60 | -6.01 | 29.37 | 2.94 | -7.97 | 24.63 |
| | CFSR | 18.55 | 21.93 | -1.20 | 20.57 | 0.65 | -0.73 | 21.05 |
| | MERRA | 12.95 | 18.90 | -12.59 | 26.64 | -2.84 | -11.31 | 8.73 |
| | OAFlux | 26.86 | 26.09 | 5.24 | 24.50 | 2.03 | 3.44 | 30.34 |

| Station | Products | Wind | Ta | SST | Ta/Wind | Ta/SST | Wind/SST | Original |
|---|---|---|---|---|---|---|---|---|
| KJ (37.62) | INTERIM | 12.06 | 12.72 | 4.41 | 11.37 | 2.44 | 2.57 | 15.61 |
| | NCEP1 | 8.33 | -4.82 | 10.92 | -4.93 | -0.97 | 14.99 | 8.12 |
| | NCEP2 | 12.19 | 5.80 | 18.28 | 0.41 | 5.63 | 13.17 | 19.94 |
| | CFSR | 9.81 | 7.32 | 3.47 | 7.66 | 0.72 | 3.74 | 11.39 |
| | MERRA | -14.86 | -13.15 | -13.54 | -4.64 | -8.11 | -7.89 | -18.34 |
| | OAFlux | 15.82 | 13.25 | 9.65 | 11.43 | 3.52 | 6.01 | 20.55 |

| Station | Products | Wind | Ta | SST | Ta/Wind | Ta/SST | Wind/SST | Original |
|---|---|---|---|---|---|---|---|---|
| DH (35.76) | INTERIM | -1.27 | 1.96 | 5.47 | -0.88 | 5.78 | 2.96 | 4.17 |
| | NCEP1 | -4.33 | -11.94 | 10.56 | -12.96 | 1.29 | 12.66 | -1.04 |
| | NCEP2 | -2.21 | -5.04 | 20.50 | -11.25 | 9.15 | 12.76 | 8.36 |
| | CFSR | -3.35 | 3.50 | 0.67 | 1.30 | 5.20 | -1.41 | 2.02 |
| | MERRA | -12.80 | -7.49 | -9.09 | -4.17 | -1.75 | -5.47 | -12.16 |
| | OAFlux | 4.50 | 0.66 | 15.99 | -3.13 | 6.97 | 11.07 | 12.15 |

| Station | Products | Wind | Ta | SST | Ta/Wind | Ta/SST | Wind/SST | Original |
|---|---|---|---|---|---|---|---|---|
| YS (30.60) | INTERIM | 2.22 | 1.04 | 1.85 | 2.14 | 1.97 | 3.23 | 0.84 |
| | NCEP1 | -8.81 | 2.39 | -11.53 | 5.01 | 0.89 | -10.24 | -10.65 |
| | NCEP2 | -8.67 | 7.43 | -10.77 | 6.23 | 4.44 | -11.35 | -8.33 |
| | CFSR | -7.45 | 10.50 | -14.51 | 11.03 | 2.47 | -13.81 | -7.90 |
| | MERRA | -8.94 | -4.91 | -9.37 | -0.28 | -2.01 | -5.42 | -12.50 |
| | OAFlux | -0.24 | 2.69 | 3.12 | 1.48 | 4.43 | 1.62 | 1.12 |

# 요약 (국문 초록)

해양-대기의 경계 면을 통한 상호 작용은 지구의 기후 시스템에 있어서 중요한 역할을 한다. 특히 잠열과 현열을 통한 해양과 대기 사이의 열 교환은 해양-대기 상호작용을 이해 하고 예측하기 위해 그 크기와 변동성에대한 정량적으로 정확한 정보를 필요로 하고 있다. 재분석장 자료는 해양과 대기 사이의 잠열 과 현열을 통한 열교환에 대해 비교적 긴 기간의, 일정한(consistent) 자료를 전구(global) 규모로 제공하여, 현재 많은 분야에서 사용 되고 있다. 다양한 종류의 재분석장 자료가 있다. 하지만 자료 동화를 통한 모델 결과 이기 때문에 모델에 의한 바이어스(bias)가 항상 존재하며 사전 검증(validation)이 반드시 이루어 져야 한다. 한반도 주변해에서는 일부 초기 재분석 장들의 상호 비교 및 검증이 이루어 졌으나 비교적 최근에 나온 재분석장 자료(CFSR, INTERIM, MERRA)를 포함해서는 이루어지지 않은 상태이다. 본 연구에서는 기상청-해양관측 부이(덕적도, 칠발도, 거문도, 거제도, 동해, 포항), 한국 해양 연구원-황해 중부 부이에서 관측된 기상자료(바람, 습도, 대기 온도, 대기압, 상대습도)와 벌크 공기 역학법 (COARE 3.0 algorithm)을 이용해 계산된 잠열과 현열을 통해 주요 재분석장 자료(NCEP1, NCEP2, CFSR, INTERIM, MERRA, OAFlux)을 비교 검증 하였다. 부이에서 계산된 자료를 기준으로 대부분의 재분석 자료는 연안에서 상당히 큰 오차를 가짐을 보였고, 이를 통해 어떠한 재분석 자료도 연안에서 잠열과 현열의 크기와 변동성을 정확히 모수화 하자 못하는 것을 확인 하였다. 벌크 공기 역학법을 하나로 통일하여 재계산한 열속을 이용해 각 재분석 자료가 가지는 기상변수에 의한 오차를 계산 하였다. 오차(systematic error)는 열속의 크기에 따라 달라 지는 경향을 보였으며, 열속이 큰 겨울철의 오차에 의해 재분석장의 총 오차의 부호와 크기가 결정 되는 것을 것을 확인 할 수 있었다. 마지막으로 민감도 테스트를 통해 각 기상 변수에 따른 오차 정도를 확인하였고 이를 통해 고해상도의 수온자료 통해 재분석장 자료가 계선 될 수 있음을 확인 하였다.